

# Optical Spectra of the Type Ia Supernova 1998aq

David Branch<sup>1</sup>, Peter Garnavich<sup>2</sup>, Thomas Matheson<sup>3</sup>, E. Baron<sup>1</sup>, R. C. Thomas<sup>1</sup>,  
Kazuhito Hatano<sup>4</sup>, Peter Challis<sup>3</sup>, S. Jha<sup>3</sup>, and Robert P. Kirshner<sup>3</sup>

Received \_\_\_\_\_; accepted \_\_\_\_\_

arXiv:astro-ph/0305321v1 18 May 2003

---

<sup>1</sup>Dept. of Physics and Astronomy, University of Oklahoma, Norman, OK 73019

<sup>2</sup>Dept. of Physics and Astronomy, University of Notre Dame, Notre Dame, IN 46556

<sup>3</sup>Harvard-Smithsonian Center for Astrophysics, 60 Garden Street, Cambridge, MA 02138

<sup>4</sup>Department of Astronomy, School of Science, University of Tokyo, Tokyo, Japan

## ABSTRACT

We present 29 optical spectra of the normal Type Ia SN 1998aq, ranging from 9 days before to 241 days after the time of maximum brightness. This spectroscopic data set, together with photometric data presented elsewhere, makes SN 1998aq one of the best observed Type Ia supernovae at optical wavelengths. We use the parameterized supernova synthetic-spectrum code **Synow** to study line identifications in the early photospheric-phase spectra. The results include evidence for lines of singly ionized carbon, at ejection velocities as low as 11,000 km s<sup>-1</sup>. Implications for SN Ia explosion models are discussed.

*Subject headings:* supernovae: general — supernovae: individual (SN 1998aq)

## 1. INTRODUCTION

The discovery in a relatively nearby galaxy of a Type Ia supernova (SN Ia), more than a week before its time of maximum brightness, presents an observational opportunity that should not be missed. A few days after the discovery of SN 1998aq in NGC 3982 on 1998 April 13 by the U.K. Supernova/Nova Patrol (Hurst, Armstrong, & Arbour 1998), photometric and spectroscopic observations undertaken at the F. L. Whipple Observatory (FLWO) revealed that the supernova was a Type Ia whose brightness was on the rise (Garnavich et al. 1998). Subsequent observations resulted in SN 1998aq becoming one of the best observed SNe Ia at optical wavelengths. The *Hubble Space Telescope* has been used by Saha et al (2001; see also Stetson & Gibson 2001) to make a Cepheid-based determination of the distance to NGC 3982, so that SN 1998aq can be added to the list of SNe Ia that are used to calibrate the extragalactic distance scale.

A preliminary report of the photometric observations of SN 1998aq has been given

by Boffi & Riess (2003), and the final results will appear elsewhere (A. G. Riess et al., in preparation). SN 1998aq reached a maximum brightness of  $B=12.39$  on 1998 April 27. The value of  $\Delta m_{15}$ , the decline of the blue-band magnitude during the first 15 days after maximum (Phillips 1993), was 1.14, a typical value for a normal SN Ia. SN 1998aq was photometrically normal, except that some of its broad-band colors were unusually blue, e.g.,  $B - V = -0.18$  at the time of  $B$  maximum.

## 2. OBSERVATIONS

Low-dispersion spectra of SN 1998aq were obtained with the FAST spectrograph (Fabricant et al. 1998) on the 1.5-m Tillinghast telescope at FLWO. The FAST spectrograph uses a  $2688 \times 512$  Loral CCD with a spatial scale of  $1.''1$  per pixel in the binning mode used for these observations. Details of the exposures are given in Table 1. The data were reduced in the standard manner with IRAF<sup>5</sup> and our own routines. The spectra were optimally extracted (Horne 1986). Wavelength calibration was accomplished with HeNeAr lamps taken immediately after each SN exposure. Small-scale adjustments derived from night-sky lines in the SN frames were also applied. Spectrophotometric standards are listed in Table 1. We attempted to remove telluric lines using the well-exposed continua of the spectrophotometric standards (Wade & Horne 1988; Matheson et al. 2001). The spectra were, in general, not taken at the parallactic angle (Filippenko 1982). For the spectra modeled in this paper, though, the airmass was low ( $< 1.2$ ).

The spectra, labelled by the epoch in days with respect to the date of maximum

---

<sup>5</sup>IRAF is distributed by the National Optical Astronomy Observatories, which are operated by the Association of Universities for Research in Astronomy, Inc., under cooperative agreement with the National Science Foundation.

brightness in the  $B$  band (1998 April 27), are displayed in Figs. 1 - 3. The spectra are those of a normal SN Ia. The early spectra, from  $-9$  to 7 days (Fig. 1), contain the characteristic deep Si II absorption near  $6100 \text{ \AA}$  and the distinctive S II W-shaped feature from about  $5200$  to  $5500 \text{ \AA}$ . The spectra between 19 and 91 days (Figs. 2 and 3) are those of a SN Ia making the transformation from the photospheric to the nebular phase. By 211 days (Fig. 3) the transformation was complete.

In Figs. 4 and 5, four spectra of SN 1998aq are compared to those of another well observed event, SN 1994D (Patat et al. 1996). The similarity of the spectra at  $-8$  days (Fig. 4) is impressive, considering that pre-maximum spectra of SNe Ia exhibit considerable diversity (e.g., Hatano et al. 2000; Li et al. 2001). At  $-8$  days the main difference is that SN 1998aq has a peak near  $4600 \text{ \AA}$  that is not present in SN 1994D; otherwise practically all of the features, including the weak ones, are quite similar. At 4, 19, and 54/55 days the spectra also are similar, although they are distinguishable, e.g., near  $4100 \text{ \AA}$  at 4 days and near  $5400 \text{ \AA}$  at 19 and 54/55 days.

In Fig. 6 the blueshifts, expressed in  $\text{km s}^{-1}$ , of the absorption near  $6100 \text{ \AA}$  produced by Si II  $\lambda 6355$  in the early spectra of SNe 1998aq and 1994D are compared. Except at the earliest times, when the blueshift is changing rapidly with time and that of SN 1994D is mildly higher than that of SN 1998aq, the differences are within the measurement errors of about  $250 \text{ km s}^{-1}$ . Fig. 7 shows the blueshifts of four absorption features in SN 1998aq that are not badly blended, and of which we are confident of the identifications (Si II  $\lambda 6355$ , Ca II  $\lambda 3945$ , S II  $\lambda 5654$ , and Si III  $\lambda 4560$ ). The blueshifts of the deep Ca II and Si II absorptions remain near  $10,000 \text{ km s}^{-1}$  even at 35 days, but those of the weaker Si III and S II features decrease more rapidly.

From Fig. 6 we estimate a value of  $10,300 \text{ km s}^{-1}$  for the  $v_{10}(\text{Si II})$  parameter — the blueshift of the deep Si II absorption 10 days after maximum brightness (Branch &

van den Bergh 1993). In the 0, 1, 2, and 3 day spectra we measure values of 0.22, 0.20, 0.22, and 0.24 for the parameter  $R(Si II)$  (Nugent et al. 1995), in good agreement with the values of  $0.22 \pm 0.02$  measured by Vinko et al. (1999) in a  $-5$  day spectrum; we recommend  $R(Si II)=0.22\pm 0.01$ . Hatano et al. (2000) showed and discussed the diversity among SNe Ia in a plot of  $R(Si II)$  versus  $v_{10}(Si II)$  (their Fig. 1). Our measured values put SN 1998aq in the most heavily populated part of their plot, near, e.g., SNe 1994D, 1996X, 1998bu, and 1990N. Garnavich et al. (2000) have shown that there is a tight relation between  $R(Si II)$  [referred to as  $R(Si II/Ti II)$  by Garnavich et al.] and  $\Delta m_{15}$ . Garnavich et al. intended to measure  $R(Si II)$  only in spectra obtained within three days of maximum light, but for SN 1998aq their adopted date of maximum differed from the date later reported by Boffi & Riess (2003). With our recommended value of  $R(Si II)$ , based on spectra obtained within three days of the revised date of maximum, SN 1998aq fits the Garnavich et al. relation between  $R(Si II)$  and  $\Delta m_{15}$  even better.

### 3. LINE IDENTIFICATIONS IN EARLY SPECTRA

The analysis of supernova spectra begins with the often difficult process of making line identifications. Only a limited number of good SN Ia spectra have been obtained well before the time of maximum light, so we are especially interested in exploring line identifications in the earliest spectrum of SN 1998aq, at  $-9$  days. For comparison we also will look at the 0 and 7 day spectra. These three spectra are compared in Fig. 8. The overall appearance of these spectra is rather similar, although some significant changes do occur during this time interval: the Si II, S II, and Ca II absorptions become deeper with time; the absorption trough from 4800 to 5000 Å in the  $-9$  day spectrum breaks up in the 7 day spectrum; and the absorption trough from 4200 to 4500 Å in the 7 day spectrum is more broken up in the  $-9$  day spectrum.

We have studied line identifications by comparing the three spectra of Fig. 8 with numerous synthetic spectra generated with the parameterized supernova synthetic-spectrum code **Synow**. This code has been used and described in several recent papers, e.g., Branch et al. (2002). The basic assumptions are spherical symmetry, a sharp photosphere, velocity proportional to radius, and resonance scattering in the Sobolev approximation. The shape of the underlying continuum is that of a blackbody at temperature  $T_{bb}$ . Line optical depths are taken to vary as  $\exp(-v/v_e)$ , with  $v_e=1000 \text{ km s}^{-1}$  for all synthetic spectra shown in this paper. For each ion whose lines are introduced, the maximum Sobolev optical depth of a reference line is a fitting parameter. Ordinarily, the maximum line optical depth is at the photosphere, but for a “detached” ion the line optical depth is zero at the photosphere and rises discontinuously to its maximum value at some higher detachment velocity. The optical depths of the other lines of an ion, relative to that of the reference line, are calculated for Boltzmann excitation at temperature  $T_{exc}$ . In this paper, instead of adopting a common value of the excitation temperature  $T_{exc}$  as the default value, the default value for each ion is the temperature at which the ion’s reference-line optical depth reaches a maximum in plots of optical depth versus temperature (Hatano et al. 1999b). This is a reasonable default since, e.g., if lines of high excitation are present they are likely to be formed in high temperature layers. The default excitation temperatures are used throughout this paper except in one instance that is mentioned below.

### 3.1. The –9 Day Spectrum

The –9 day spectrum is shown in Fig. 9, with the measured wavelengths of absorption features labelled, so that we can conveniently refer to each absorption throughout this subsection. In this and all subsequent figures of this paper, instead of plotting  $f_\nu$  on the vertical axis we plot  $f_\nu/\nu$ , to make the spectrum approximately flat. This provides a better

view of features at the longer wavelengths where the underlying continuum is low, which is helpful because the diagnostic value of a spectral feature is not proportional to the level of the underlying continuum. Note also that in order to show as much detail as possible, in this and subsequent figures the flux axis does not go to zero.

In Fig. 10 the same  $-9$  day spectrum is compared with a synthetic spectrum that has  $v_{phot} = 13,000 \text{ km s}^{-1}$ ,  $T_{bb}=16,000 \text{ K}$ , and includes lines of seven ions. The ion-specific parameters of the synthetic spectrum are listed in Table 2. The fit shown in Fig. 10 is good by supernova standards, although there are two significant discrepancies that we have not yet resolved: the synthetic spectrum is too high from  $4460$  to  $4580 \text{ \AA}$ , and too low from  $4000$  to  $4160 \text{ \AA}$ . The contributions of each ion to the synthetic spectrum of Fig. 10 are shown in Figs. 11 to 17, each of which we now briefly discuss.

Fig. 11 shows that the main contribution of Si II is that  $\lambda 6355$  accounts for almost all of the  $6115 \text{ \AA}$  absorption. Note that  $\lambda 6355$  produces a synthetic emission peak where an absorption feature is observed. The  $\lambda 5972$  and  $\lambda 5051$  lines contribute to the  $5740$  and  $4870 \text{ \AA}$  absorptions. The  $\lambda 4130$  line contributes to the  $3970 \text{ \AA}$  absorption, but absorption by  $\lambda 4130$  also is partially responsible for our failure to fit the observed emission peak near  $4070 \text{ \AA}$ . In any case, the presence of Si II  $\lambda 6355$  in the  $-9$  day spectrum of SN 1998aq is, of course, definite.

Fig. 12 shows that the main contribution of S II is that  $\lambda 5654$  and  $5468$  produce the  $5420$  and  $5260 \text{ \AA}$  absorptions. Lines near  $\lambda 6305$  make a minor contribution to the  $6115 \text{ \AA}$  absorption. The  $\lambda 5208$  line may be responsible for the  $5110 \text{ \AA}$  absorption, although it does not produce a distinct absorption in the full synthetic spectrum of Fig. 10. The  $\lambda 5032$  line contributes to the  $4870 \text{ \AA}$  absorption and some weaker S II lines make minor contributions. The  $\lambda 4163$  line is partially responsible for our failure to fit the observed emission peak near  $4070 \text{ \AA}$ . Nevertheless, the presence of S II  $\lambda 5654$  and  $5468$  is definite.

Fig. 13 shows that the only contribution of Ca II (since the spectrum does not extend to the infrared triplet) is that  $\lambda 3945$  (the H&K lines) produces the  $3805 \text{ \AA}$  absorption. The presence of Ca II  $\lambda 3945$  is definite.

Fig. 14 shows that Si III  $\lambda 4560$  produces the  $4390 \text{ \AA}$  absorption. It is likely that  $\lambda 5743$  is responsible for the  $5515 \text{ \AA}$  absorption, although in Fig. 10 the synthetic absorption is at a slightly shorter wavelength than the observed one. We are confident of the presence of Si III  $\lambda 4560$ .

Fig. 15 shows that Fe III  $\lambda 5156$  and  $4420$  are largely responsible for the  $4930$  and  $4255 \text{ \AA}$  absorptions. Lines near  $\lambda 6000$  also contribute to the  $5740 \text{ \AA}$  absorption. This is the one instance in this paper where we depart from the default excitation temperature. At the Fe III default value of  $14,000 \text{ K}$  the feature produced by  $\lambda 6000$  is present but weaker. We use  $16,000 \text{ K}$  to show that Fe III might be mainly responsible for the  $5740 \text{ \AA}$  absorption at this epoch. In any case, we are confident of the presence of Fe III  $\lambda 5156$  and  $4420$ .

Fig. 16 shows the contribution of Fe II lines, detached at  $20,000 \text{ km s}^{-1}$ . This means that in the synthetic spectrum, the Fe II optical depths are zero between the velocity at the photosphere,  $13,000 \text{ km s}^{-1}$ , and the detachment velocity of  $20,000 \text{ km s}^{-1}$ . The presence of detached, high-velocity Fe II in SN 1994D was suggested by Hatano et al. (1999a) on the basis of **Synow** synthetic spectra and then supported by Lentz et al. (2001b) who carried out non-local-thermodynamic-equilibrium (NLTE) calculations with the PHOENIX code. In Fig. 16, we see that Fe II  $\lambda 5169$ ,  $5018$ , and  $4924$ , are contributing to the  $4870$ ,  $4730$ , and  $4640 \text{ \AA}$  absorptions, respectively. Lines near  $\lambda 4549$  and  $4025$  contribute to the  $4295$  and  $3970 \text{ \AA}$  absorptions. High-velocity Fe II makes a positive contribution to the full fit in Fig. 10, and we consider its presence in the observed spectrum to be likely.

Fig. 17 shows the contributions of C II lines, slightly detached at  $14,000 \text{ km s}^{-1}$ . The strongest line,  $\lambda 6580$ , is playing an important role in the synthetic spectrum: it beats down



the unwanted emission component of Si II  $\lambda 6355$ , and combines with it in the full synthetic spectrum of Fig. 10 to produce a feature near the observed 6310 Å absorption. The  $\lambda 7234$  line produces the 6940 Å absorption. (Fig. 17 is a good example of the benefit of plotting  $f_\nu/\nu$ : it gives a better view of the features produced by  $\lambda 6580$  and  $\lambda 7234$ .) The  $\lambda 4267$  line is at the right wavelength to be consistent with the 4120 Å absorption, although  $\lambda 4267$  does not produce a distinct feature in the full synthetic spectrum of Fig. 10. We consider the presence of C II lines to be likely.

### 3.2. The 0 and 7 Day Spectra

In Fig. 18 the 0 day spectrum of SN 1998aq is compared with a synthetic spectrum that has  $v_{phot}=11,000$  km s<sup>-1</sup>,  $T_{bb}=16,000$  K, and contains lines of the same seven ions that were used for the -9 day spectrum. The ion-specific parameters of the synthetic spectrum are listed in Table 3. The Fe II lines now are detached at 18,000 rather than 20,000 km s<sup>-1</sup>, and Si II and S II are mildly detached at 12,000 km s<sup>-1</sup>. Compared to the synthetic spectrum for -9 days, the Ca II line optical depths are increased by a factor of five, those of Si II and Fe III are up by small factors, the Fe II optical depths are unchanged, and those of S II, Si III, and C II are down by small factors. The overall fit in Fig. 18 is good, the main discrepancies being that the synthetic spectrum again lacks the 4070 Å emission peak, and now the synthetic spectrum is too low from 5800 to 6000 Å. The difference in the heights of the apparent continuum levels at wavelengths longer than 6500 Å has been encountered in previous **Synow** studies of SNe Ia and probably is caused by our use of a blackbody continuum.

In Fig. 18, C II  $\lambda 6580$  again beats down the Si II  $\lambda 6355$  emission and produces an absorption notch that may correspond to an observed feature. The  $\lambda 7234$  line produces a wiggle in the synthetic spectrum that may be at least partially responsible for the knee in

the observed spectrum near 7000 Å.

In Fig. 19 the 7 day spectrum of SN 1998aq is compared with a synthetic spectrum that has  $v_{phot}=11,000$  km s<sup>-1</sup> and  $T_{bb}=16,000$  K. The ion-specific parameters of the synthetic spectrum are listed in Table 4. This synthetic spectrum contains lines of six of the seven ions used previously, Si III now being omitted. Fe II has two components: one detached at 18,000 km s<sup>-1</sup> as in the 0 day spectrum, and now also an undetached component. Compared to the 0 day spectrum, the optical depths of the Si II, S II, Ca II, C II, and Fe II lines have been increased while Fe III has been decreased. The synthetic spectrum of Fig. 19 also includes contributions from Mg II, Na I, Co II, and Ti II lines, but their contributions are not major and we do not consider their presence in the observed spectrum to be established. To the extent to which we have been able to account for it, the breakup of the 4800 to 5000 Å region and the filling in of the 4200 to 4500 Å region, both mentioned above in the discussion of Fig. 8, are caused by the emergence of the undetached Fe II component. The main discrepancy in Fig. 19 is that the synthetic spectrum is too low in the interval 5100 to 6000 Å.

In Fig. 19, C II  $\lambda 6580$  leads to a (perhaps fortuitously) good fit at the top of the Si II  $\lambda 6355$  emission, and again  $\lambda 7234$  produces a feature that appears to be responsible for the observed one near 7000 Å.

#### 4. DISCUSSION

The identification of lines of Si II, S II, Ca II, Fe III, and Si III in early spectra of SNe Ia is not new, but the figures of this paper clearly illustrate the extent to which lines of these ions can account, with simple assumptions, for the observed spectral features in SN 1998aq. It is instructive to compare parameterized **Synow** spectrum fits with NLTE

synthetic spectra for specific explosion models. Lentz et al. (2001b) used the **PHOENIX** code to make detailed calculations of spectra of the deflagration model W7 (Nomoto, Thielemann, & Yokoi 1984) and found reasonably good agreement with the early spectra of SN 1994D, which as we have seen in §2 was spectroscopically similar to SN 1998aq. Fig. 20 is like Fig. 10 but also including the **PHOENIX** spectrum of model W7 at 11 days after explosion (corresponding to about 9 days before maximum light). The model W7 spectrum does have peaks and dips at some of the right wavelengths, but there is room for improvement. For example, the W7 spectrum lacks the 4390 Å absorption that we attribute to Si III  $\lambda$ 4560, and the W7 emission peaks near 5900 and 6400 Å are too high. Ongoing work involving close comparative studies of observed spectra, **Synow**-level synthetic spectra, and **PHOENIX**-level spectra of explosion models will provide indications of how explosion models need to be altered to give better agreement with observed spectra.

Apparently, Fe II features forming at high velocity,  $\geq 18,000$  km s<sup>-1</sup>, are present at the three epochs we have studied. Hatano et al. (1999a) identified high-velocity ( $\geq 20,000$  km s<sup>-1</sup>) Ca II and Fe II lines in SN 1994D. Kasen et al. (2003) discuss high-velocity (18,000 to 25,000 km s<sup>-1</sup>) components of the Ca II infrared triplet in flux and polarization spectra of SNe 2001el, and Thomas et al. (2003) discuss high-velocity ( $\geq 23,000$  km s<sup>-1</sup>) Ca II in flux spectra of the peculiar SN 2000cx. Both Kasen et al. and Thomas et al. conclude that the Ca II features formed in non-spherical geometry, probably in clumps located in front of the photosphere. The spectra of SN 1998aq do not extend to the Ca II infrared triplet (and barely extend to the high-velocity side of the Ca II H&K feature) so we have not established the presence of high-velocity Ca II features in SN 1998aq. In any case, the presence of high-velocity features in early spectra of SNe Ia evidently is not uncommon. Further studies of early-time polarization and flux spectra of SNe Ia are needed to clarify the composition, geometry, and origin of the high-velocity matter.

Perhaps the most significant result of our analysis of SN 1998aq is the evidence for C II lines. The possible presence of C II in early spectra of SNe Ia has been discussed before. For instance, Mazzali (2001) tentatively attributed absorptions in a  $-14$  day spectrum of SN 1990N to C II  $\lambda 6580$  and  $\lambda 7234$  forming near the photospheric velocity of about  $16,000$  km s $^{-1}$ . The features that we attribute to  $\lambda 6580$  and  $\lambda 7234$  in SN 1998aq are conspicuous in our figures because of we plot  $f_\nu/\nu$  to raise the red end of the spectra. If C II is present in SN 1998aq then it also is present in at least some of the other SNe Ia that have been observed at early times; e.g., similar features can be seen in spectra of SN 1994D (Fig. 4) and SN 1996X (Salvo et al. 2001).

The presence of C II would have important implications for SN Ia explosion models. In the synthetic spectrum of Fig. 10, we use C II detached at  $14,000$  km s $^{-1}$ , but in Figs. 18 and 19, C II is undetached and therefore forming down to the photospheric velocity of  $11,000$  km s $^{-1}$ , and we have not established the *absence* of carbon at even lower velocities. Published delayed–detonation models for normal SNe Ia have very little carbon below about  $30,000$  km s $^{-1}$ . Model W7, a parameterized one–dimensional (1D) deflagration model, has unburned carbon down to  $14,000$  km s $^{-1}$ . Recently computed 3D deflagrations (Khokhlov 2000; Gamezo et al. 2003) have carbon at *all* ejection velocities. The spectroscopic appearance of such models has begun to be explored (Baron et al. 2003). In the context of existing models, the presence of C II lines may be consistent with deflagrations but not with delayed–detonations. However, the spectra of 3D deflagration models appear to be inconsistent with SN Ia spectra in other respects (Thomas et al. 2002; Gamezo et al. 2003), while delayed–detonations have been found to be consistent with certain unusual SNe Ia (Lentz et al. 2001a) and in some respects with normal SNe Ia (Wheeler et al 1998). Much further work on comparing synthetic spectra, both parameterized and detailed, with observed spectra of SNe Ia is needed to guide us towards satisfactory explosion models.

This work has been supported by NSF grants AST-9986965 and AST-0204771 and NASA grant NAG5-12127.

## REFERENCES

- Baron, E., Lentz, E. J., & Hauschildt, P. H. 2003, *ApJ*, in press
- Boffi, F. R. & Riess, A. G. 2003, in *Symbiotic Stars Probing Stellar Evolution*, eds. R. L. M. Corrdai, J Mikolajewska, & T. J. Mahoney (San Francisco, ASP), in press
- Branch, D. & van den Bergh, S. 1993, *AJ*, 105, 2231
- Branch, D. et al. 2002, *ApJ*, 566, 1005
- Fabricant, D., Cheimets, P., Caldwell, N., & Geary, J. 1998, *PASP*, 110, 79
- Filippenko, A. V. 1982, *PASP*, 94, 715
- Gamezo, V., Khokhlov, A., Oran, E., Chtchelkanova, A., Rosenberg, R. 2003, *Science*, 299, 77
- Garnavich, P. et al. 1998, *IAU Circ. No. 6880*
- Garnavich, P. M. et al. 2000 (*astro-ph/0105490*)
- Hatano, K., Branch, D., Fisher, A., Baron, E., & Filippenko, A. V. 1999a, *ApJ*, 525, 881
- Hatano, K., Branch, D., Fisher, A., Millard, J., & Baron, E. 1999b, *ApJS*, 121, 233
- Hatano, K., Branch, D., Lentz, E.J., Baron, E., Filippenko, A. V., & Garnavich, P. M. 2000, *ApJ*, 543, L49
- Horne, K. 1986, *PASP*, 98, 609
- Hurst, G. M., Armstrong, M., & Arbour, R. 1998, *IAU Circ. No. 6875*
- Kasen, D. et al. 2003, *ApJ*, in press (*astro-ph/0301312*)
- Khokhlov, A. 2000, (*astro-ph/0008463*)
- Lentz, E. J., Baron, E., Branch, D., & Hauschildt, P. H. 2001a, *ApJ*, 547, 908
- Lentz, E. J., Baron, E., Branch, D., & Hauschildt, P. H. 2001b, *ApJ*, 557, 266

- Li, W. et al. 2001, *ApJ*, 546, 734
- Matheson, T., Filippenko, A. V., Ho, L. C., Barth, A. J., & Leonard, D. C. 2000, *AJ*, 120, 1499
- Mazzali, P. A. 2001, *MNRAS*, 321, 341
- Nomoto, K., Thielemann, F.-K., & Yokoi, K. 1984, *ApJ*, 286, 644
- Nugent, P., Phillips, M. M., Baron, E., Branch, D., & Hauschildt, P. 1995, *ApJ*, 455, L147
- Patat, F., Benetti, S., Cappellaro, E., Danziger, I. J., Della Valle, M., Mazzali, P. M., & Turatto, M. 1996, *MNRAS*, 278, 111
- Phillips, M. M. 1993, *ApJ*, 413, L105
- Saha, A., Sandage, A., Tammann, G. A., Dolphin, A. E., Christensen, J., Panagia, N., & Macchetto, F. D. 2001, *ApJ*, 562, 314
- Salvo, M. E., Cappellaro, E., Mazzali, P. A., Benetti, S., Danziger, I. J., Patat, F., & Turatto, M. 2001, *MNRAS*, 321, 254
- Stetson, P. M. & Gibson, B. K. 2001, *MNRAS*, 328, 1
- Thomas, R. C., Kasen, D., Branch, D., & Baron, E. 2002, *ApJ*, 567, 1037
- Thomas, R. C., Branch, D., & Baron, E., Nomoto, K., Li, W., & Filippenko, A. V. 2003, *ApJ*, submitted (astro-ph/0302260)
- Wade, R. A., & Horne, K. D. 1988, *ApJ*, 324, 411
- Wheeler, J. C., Höflich, P., Harkness, R. P., & Spyromilio, J. 1998, *ApJ*, 496, 908
- Vinkó, J., Kiss, L. L., Thomson, J., Furész, G., Lu, W., Kaszás, G., & Balog, Z. 1999, *A&A*, 345, 592

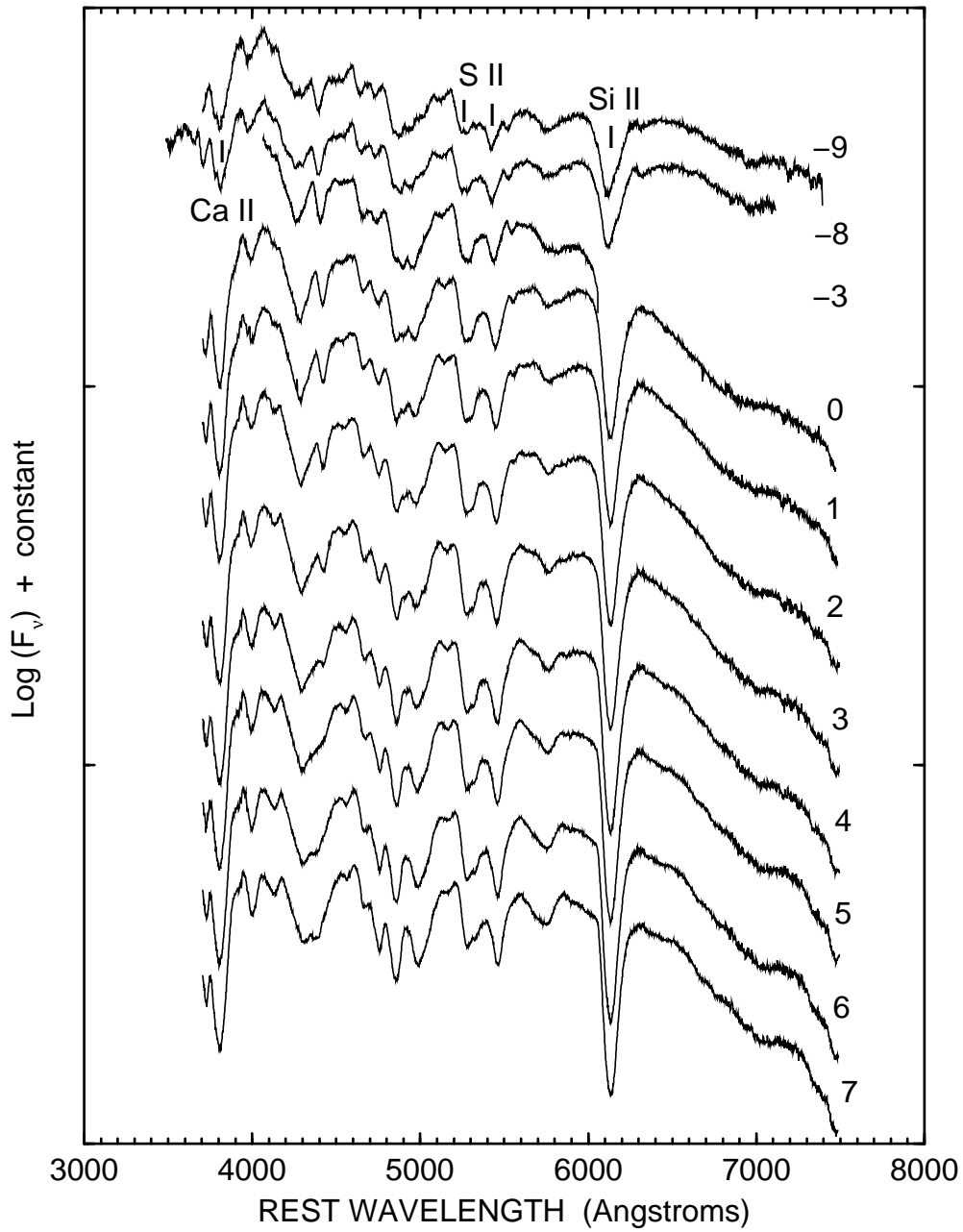


Fig. 1.— Spectra of SN 1998aq. Epochs are in days with respect to the date of maximum brightness in the  $B$  band, 1998 April 27. The vertical displacement is arbitrary. All spectra shown in this paper have been corrected for the redshift of NGC 3982,  $z = 0.003699$ . No correction for interstellar reddening has been applied.



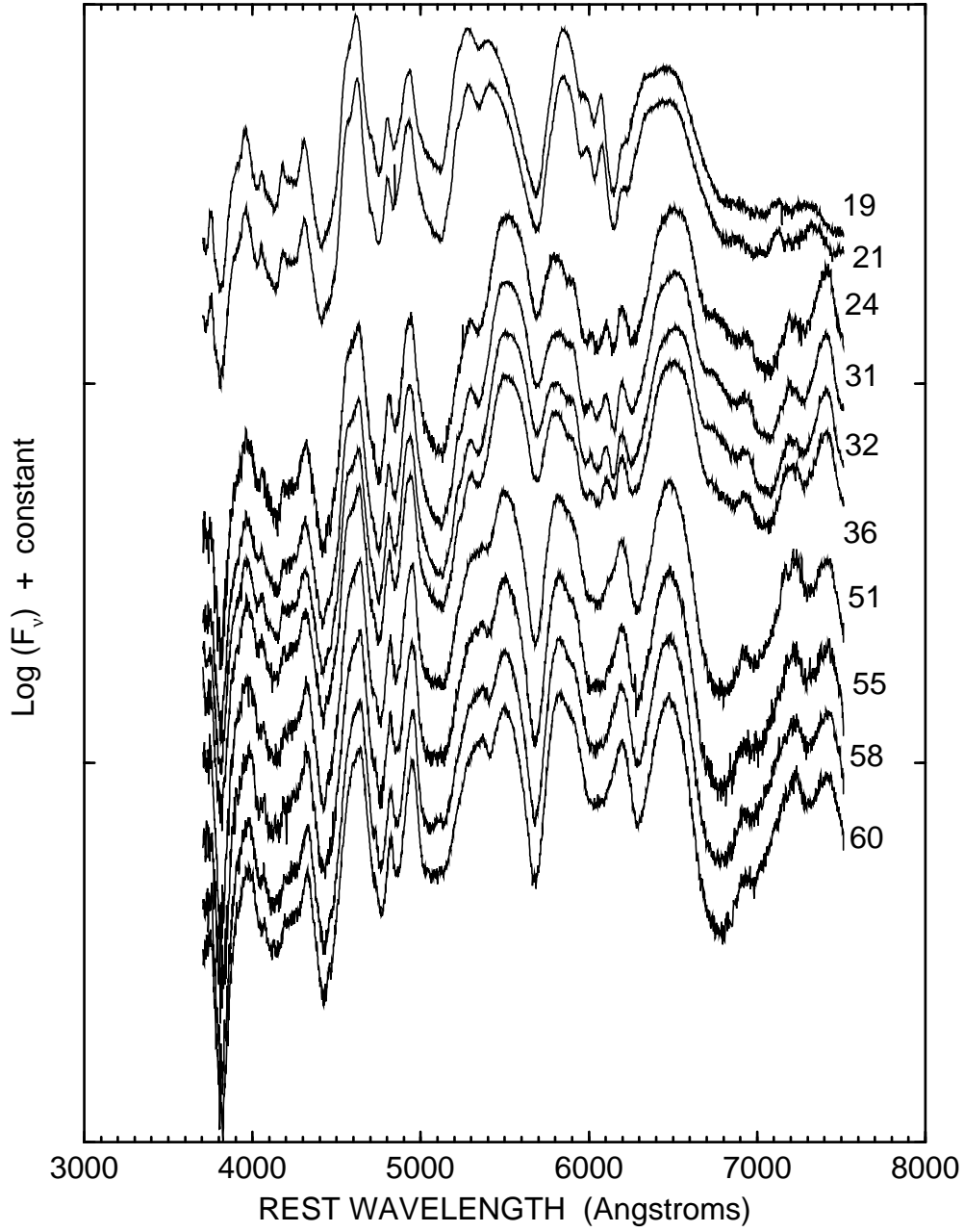


Fig. 2.— Spectra of SN 1998aq.

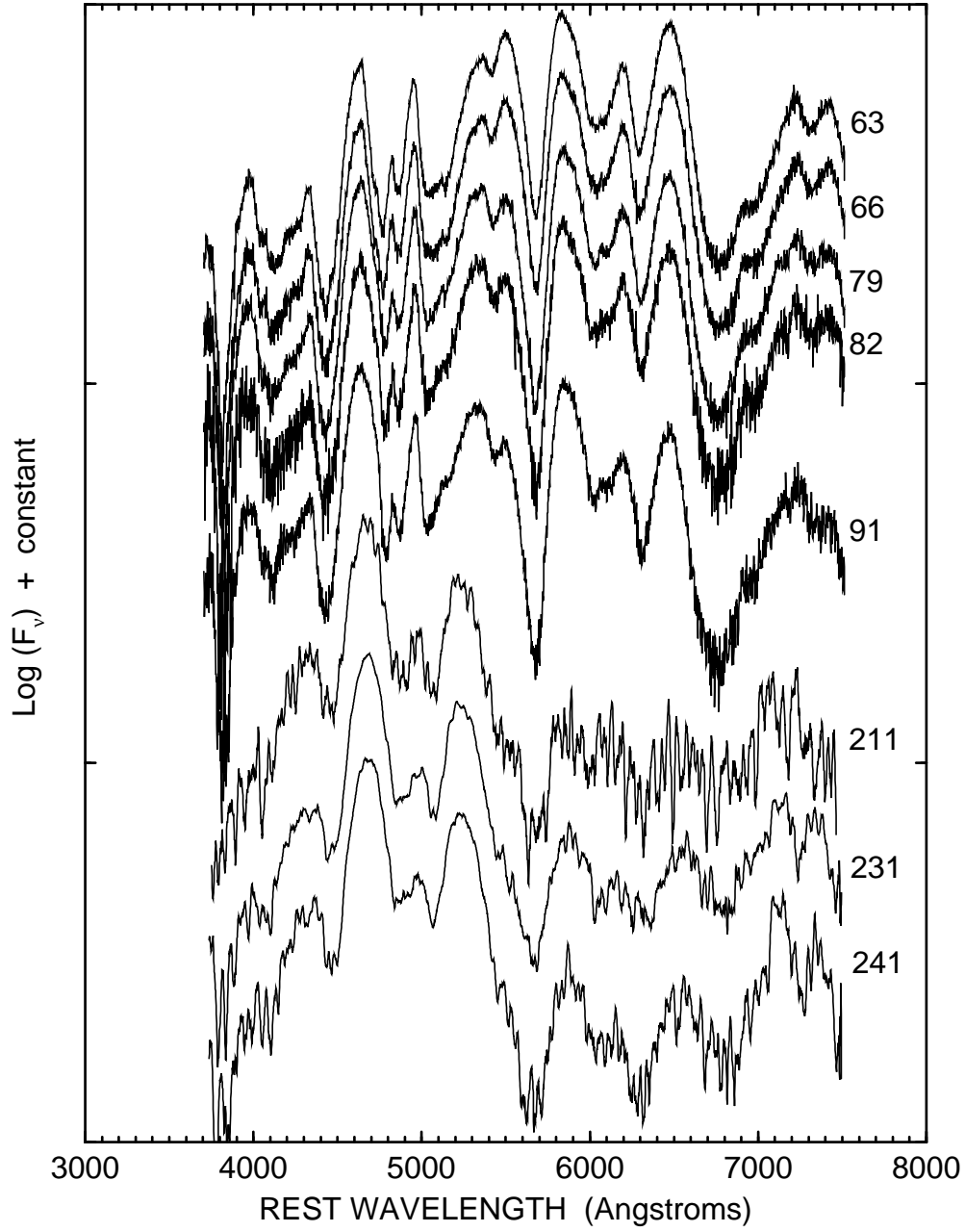


Fig. 3.— Spectra of SN 1998aq.

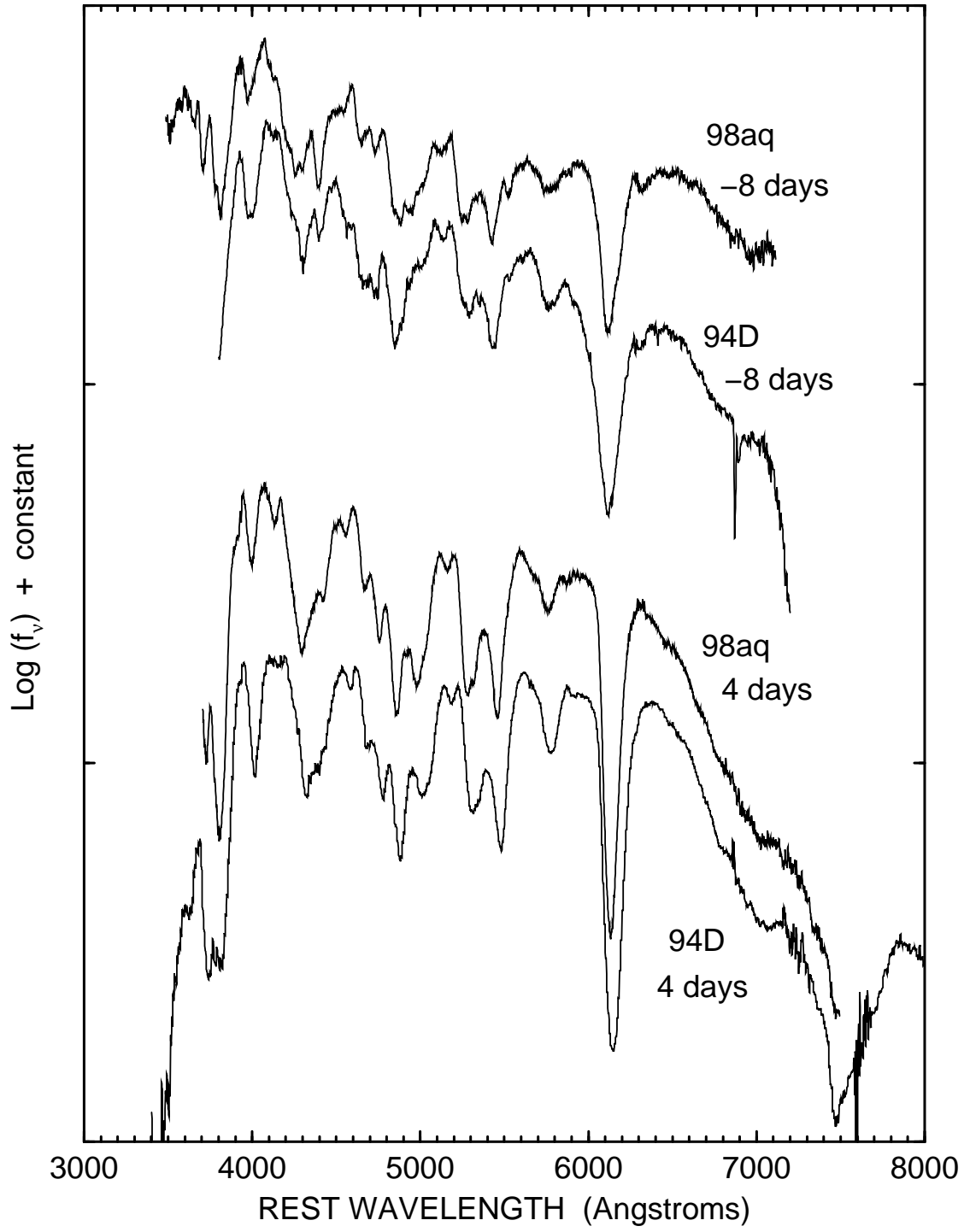


Fig. 4.— Comparisons of spectra of SNe 1998aq and 1994D.

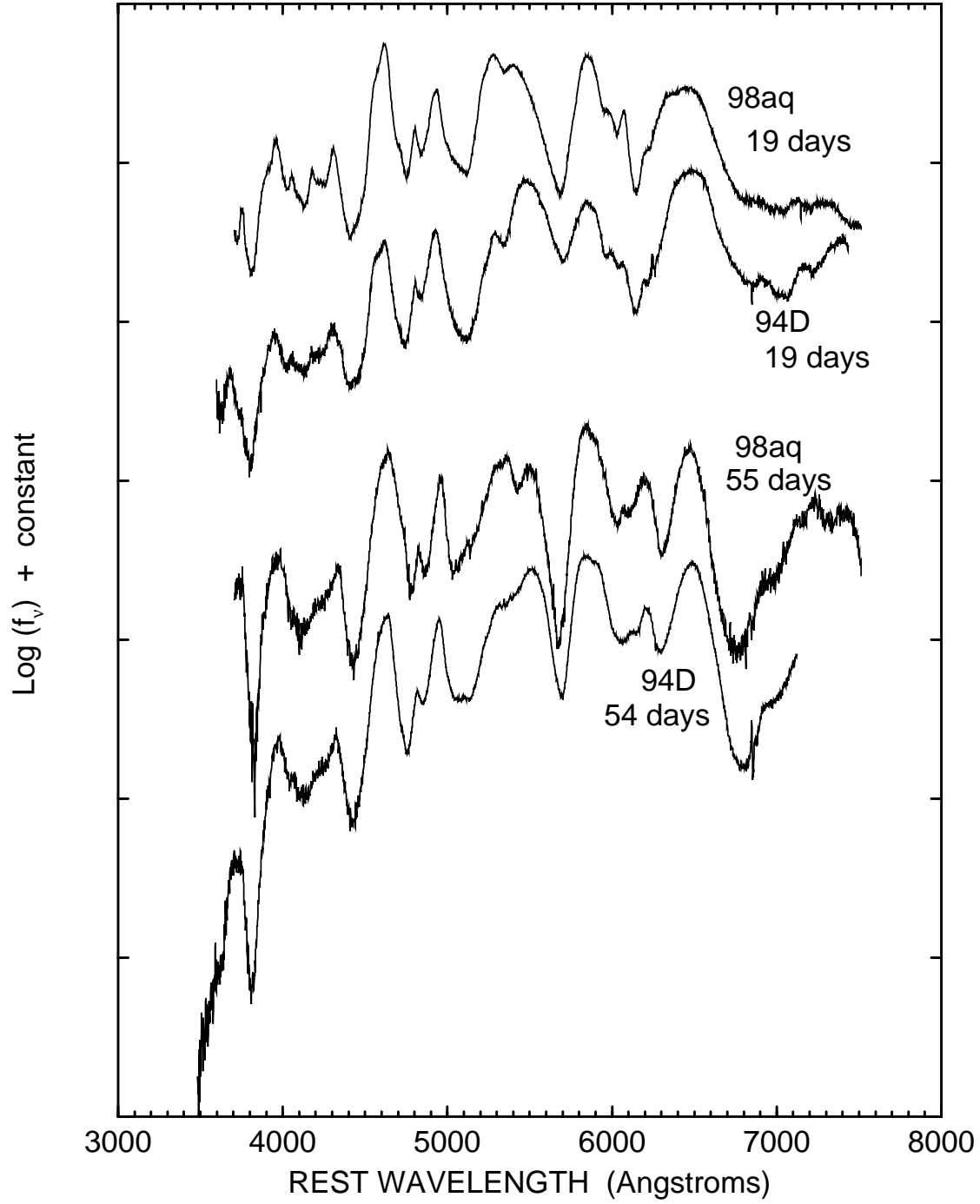


Fig. 5.— Comparisons of spectra of SNe 1998aq and 1994D.

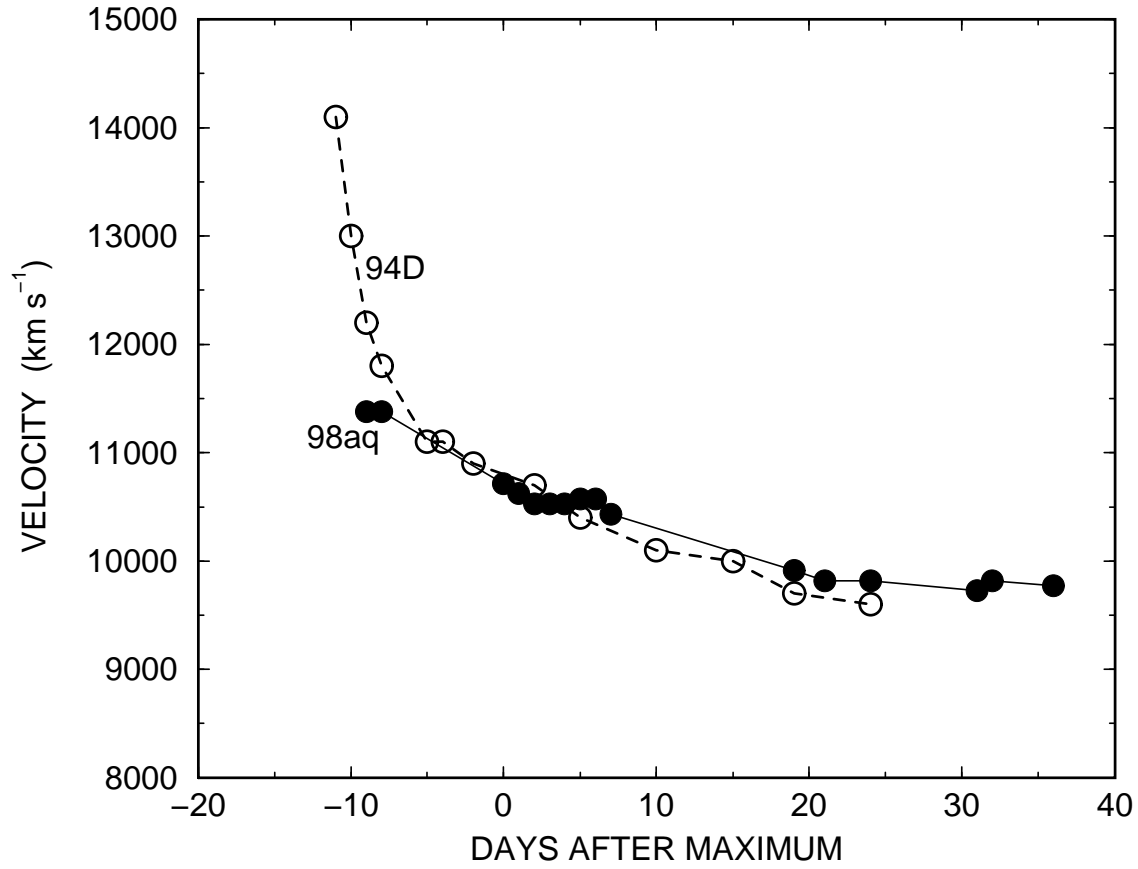


Fig. 6.— Comparison of Si II blueshifts in SNe 1998aq and 1994D.

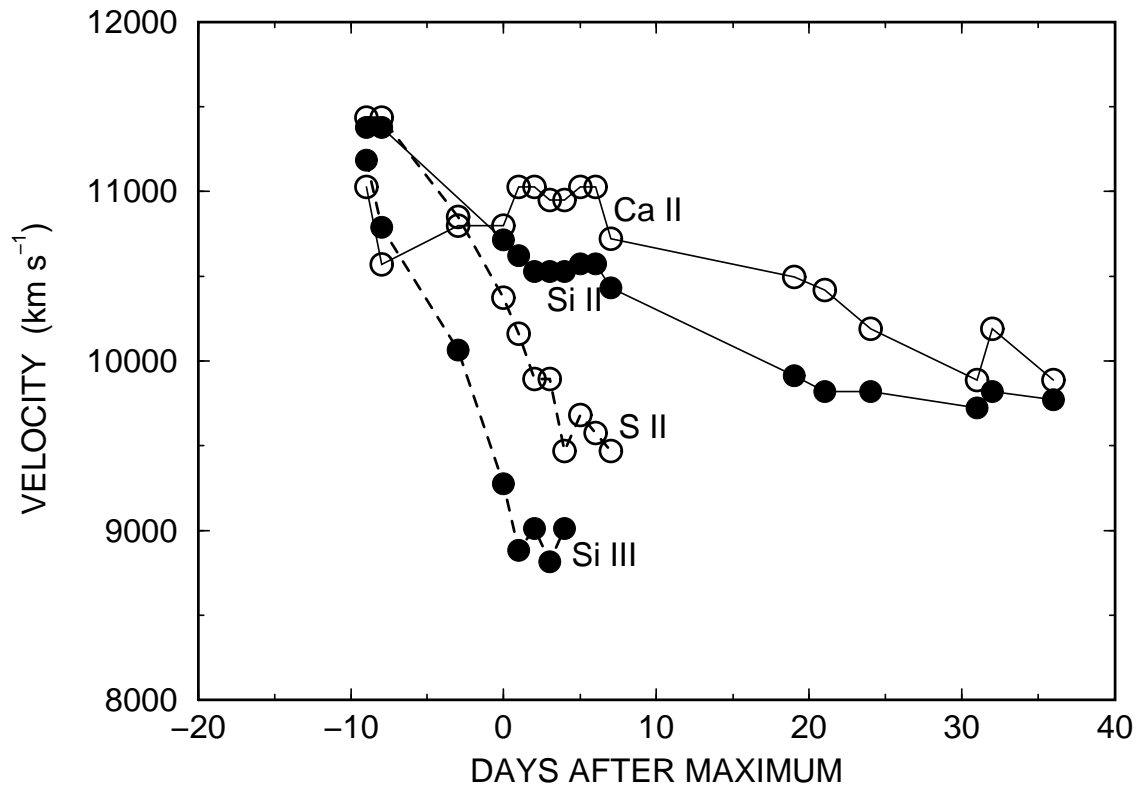


Fig. 7.— Blueshifts of four absorption features in SN 1998aq.

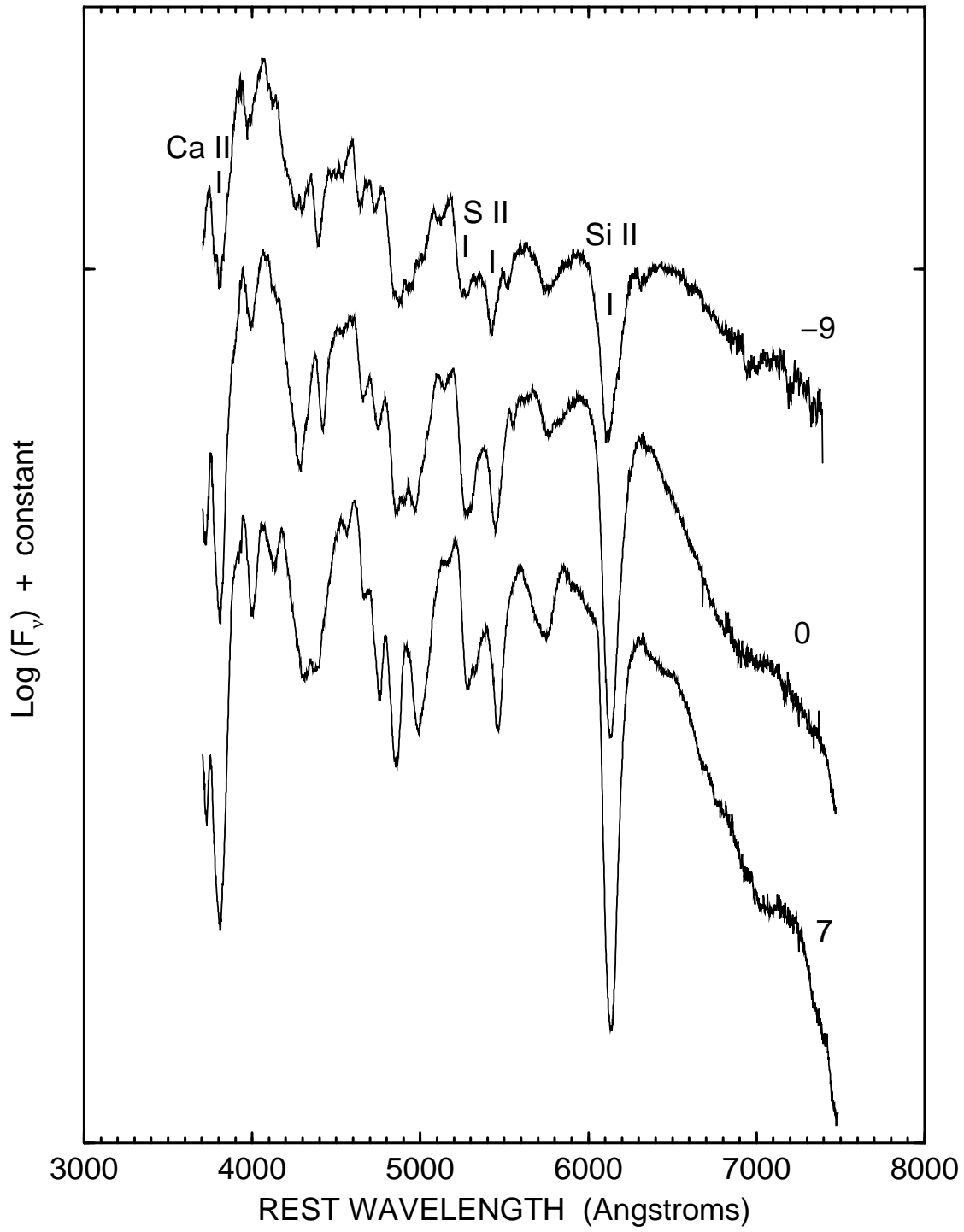


Fig. 8.— Three early spectra of SN 1998aq.

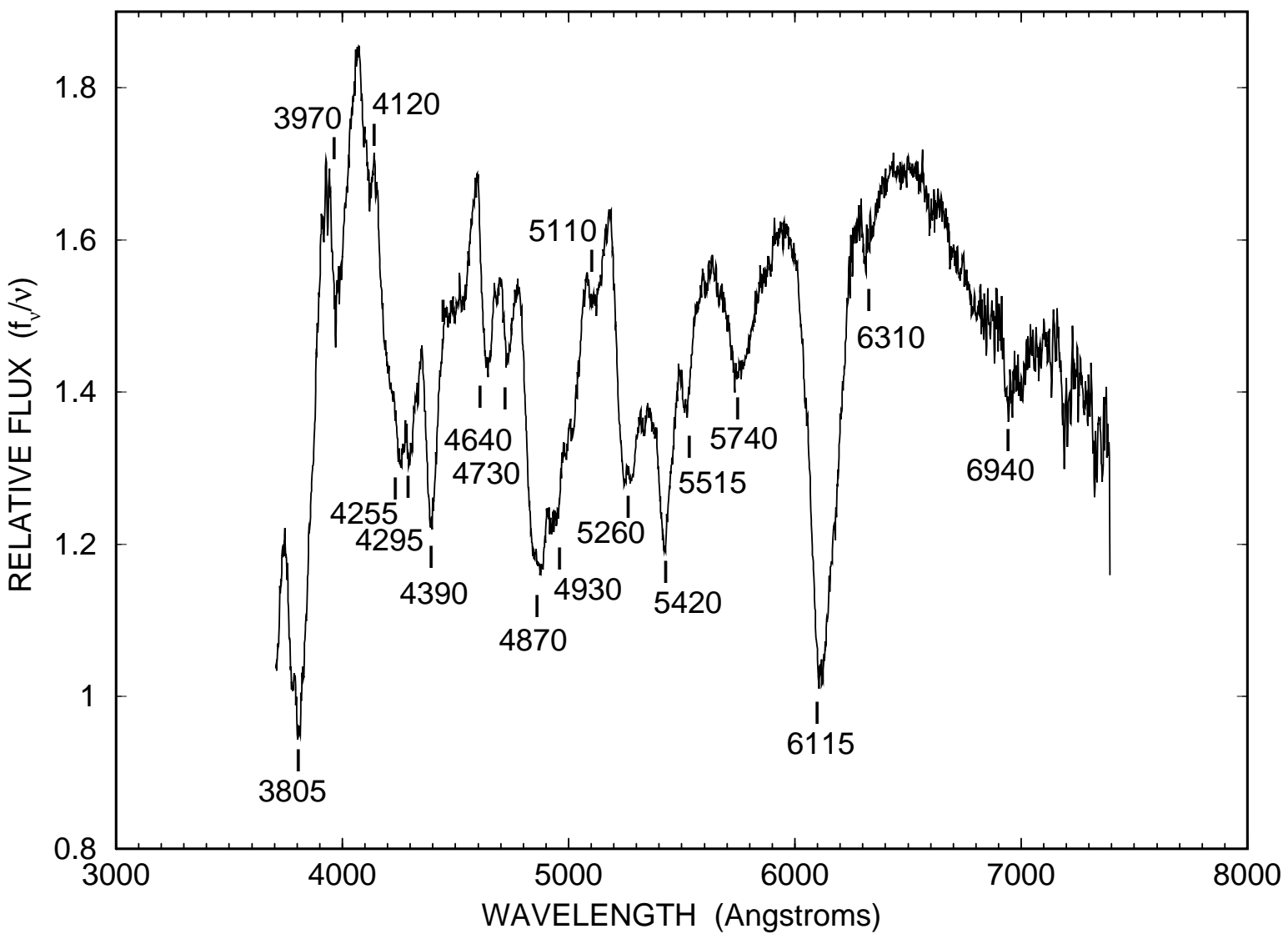


Fig. 9.— Absorption features in the  $-9$  day spectrum of SN 1998aq. Note that in this and subsequent figures the vertical axis is  $f_\nu/\nu$ .



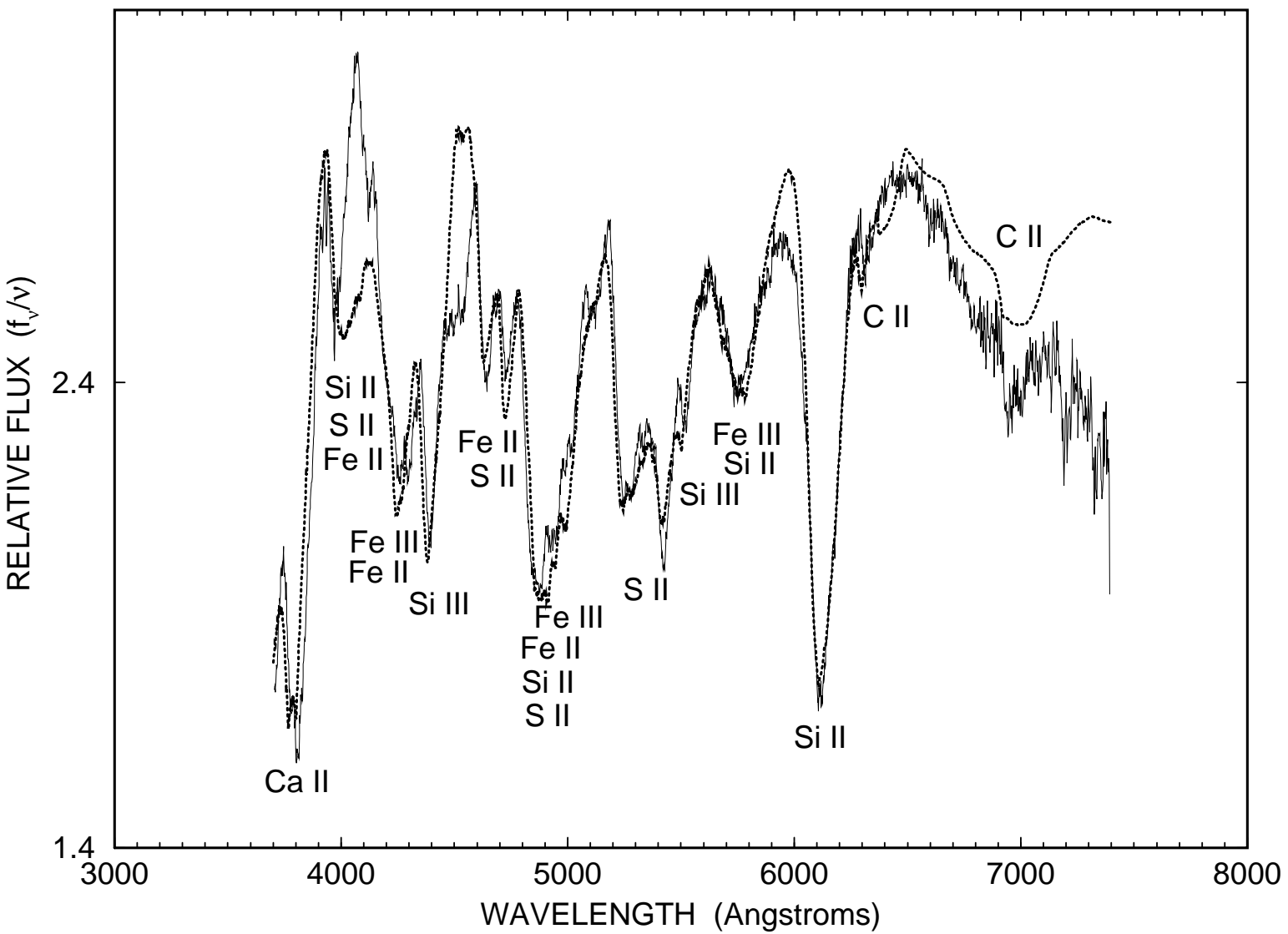


Fig. 10.— Comparison of the  $-9$  day spectrum of SN 1998aq with a **Synow** synthetic spectrum that has  $v_{phot} = 13,000$  km s $^{-1}$ ,  $T_{bb} = 18,000$ , and contains lines of seven ions.

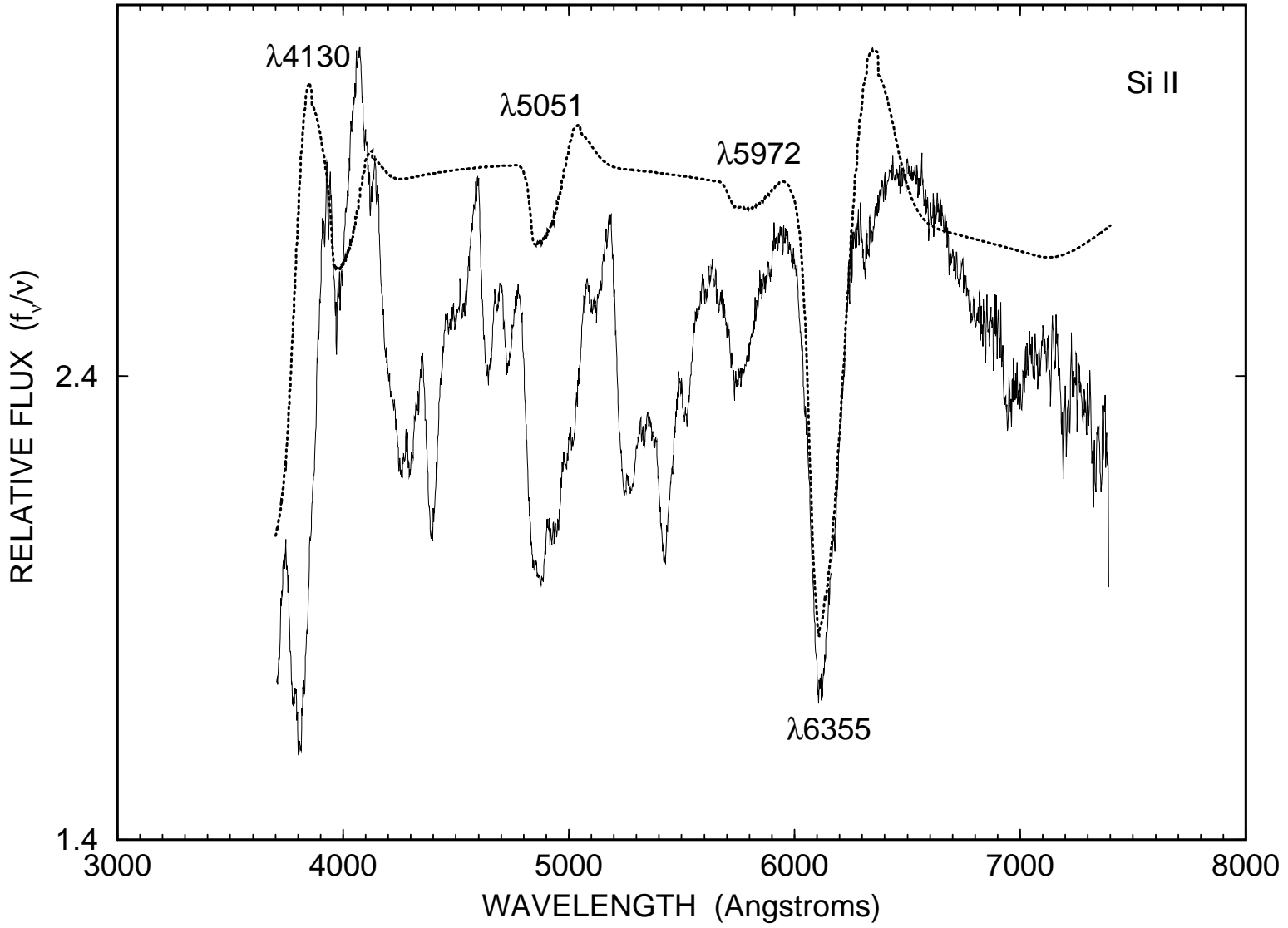


Fig. 11.— Like Fig. 10 but with only lines of Si II in the synthetic spectrum.

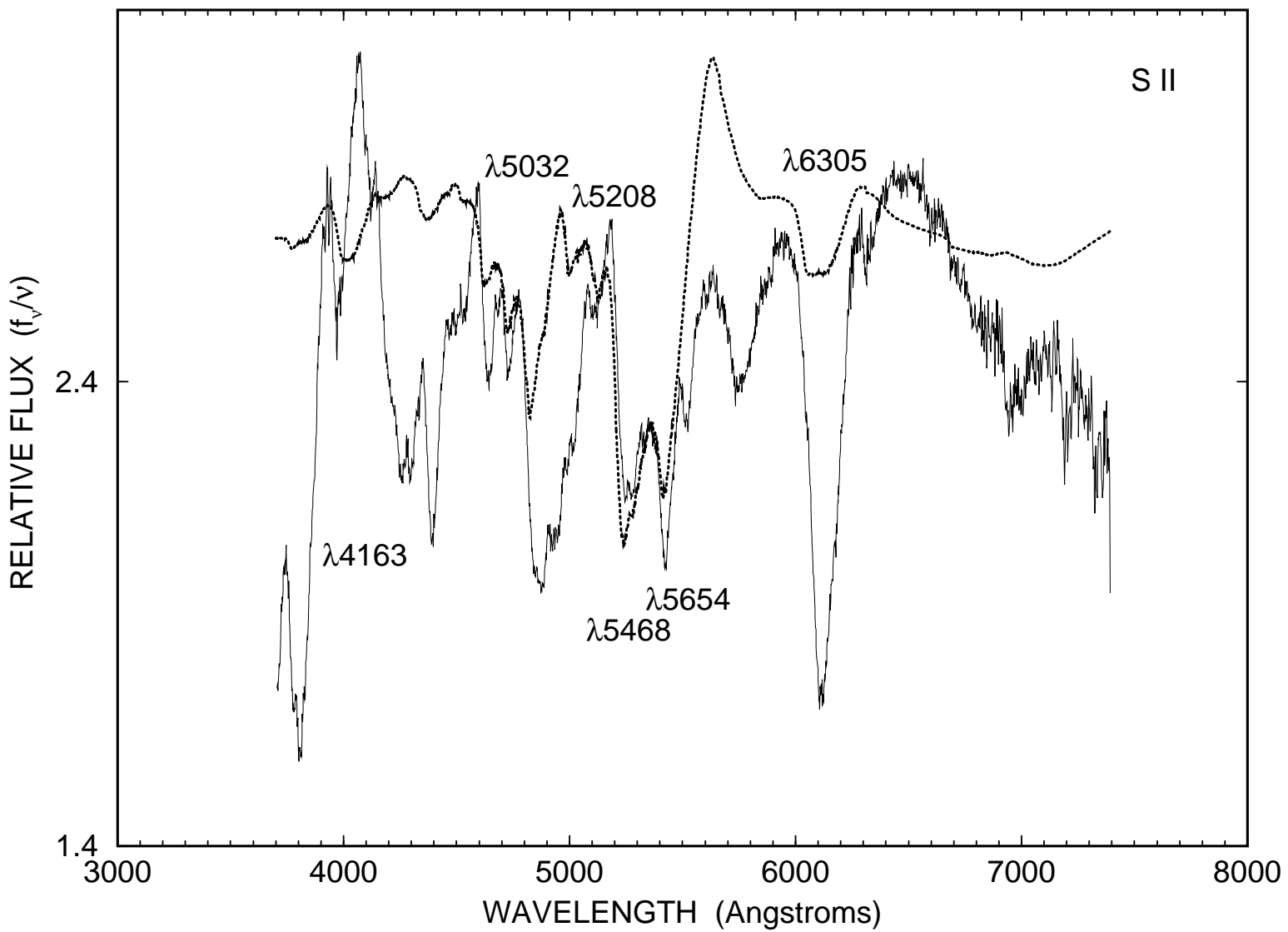


Fig. 12.— Like Fig. 10 but with only lines of S II in the synthetic spectrum.

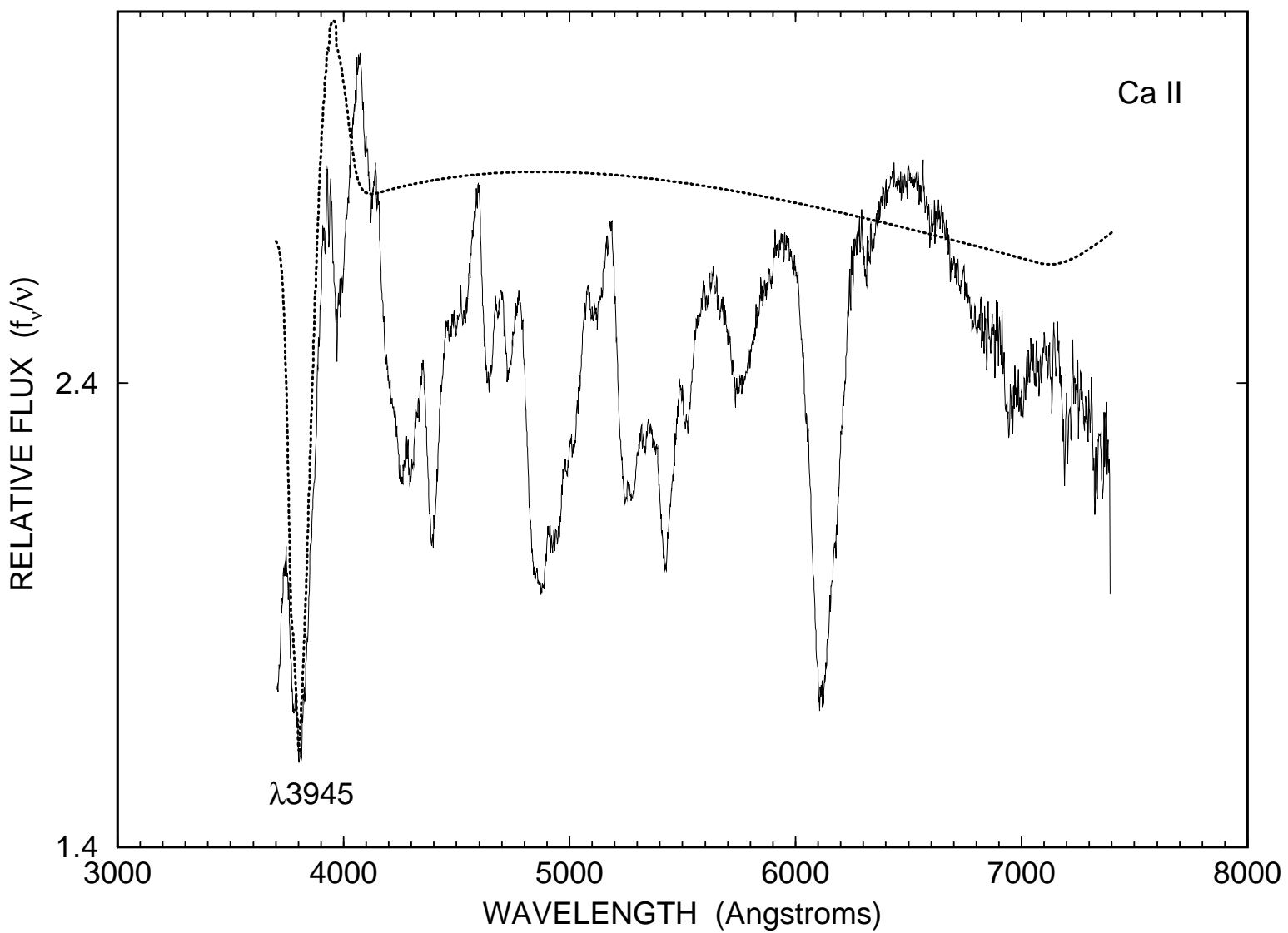


Fig. 13.— Like Fig. 10 but with only lines of Ca II in the synthetic spectrum.

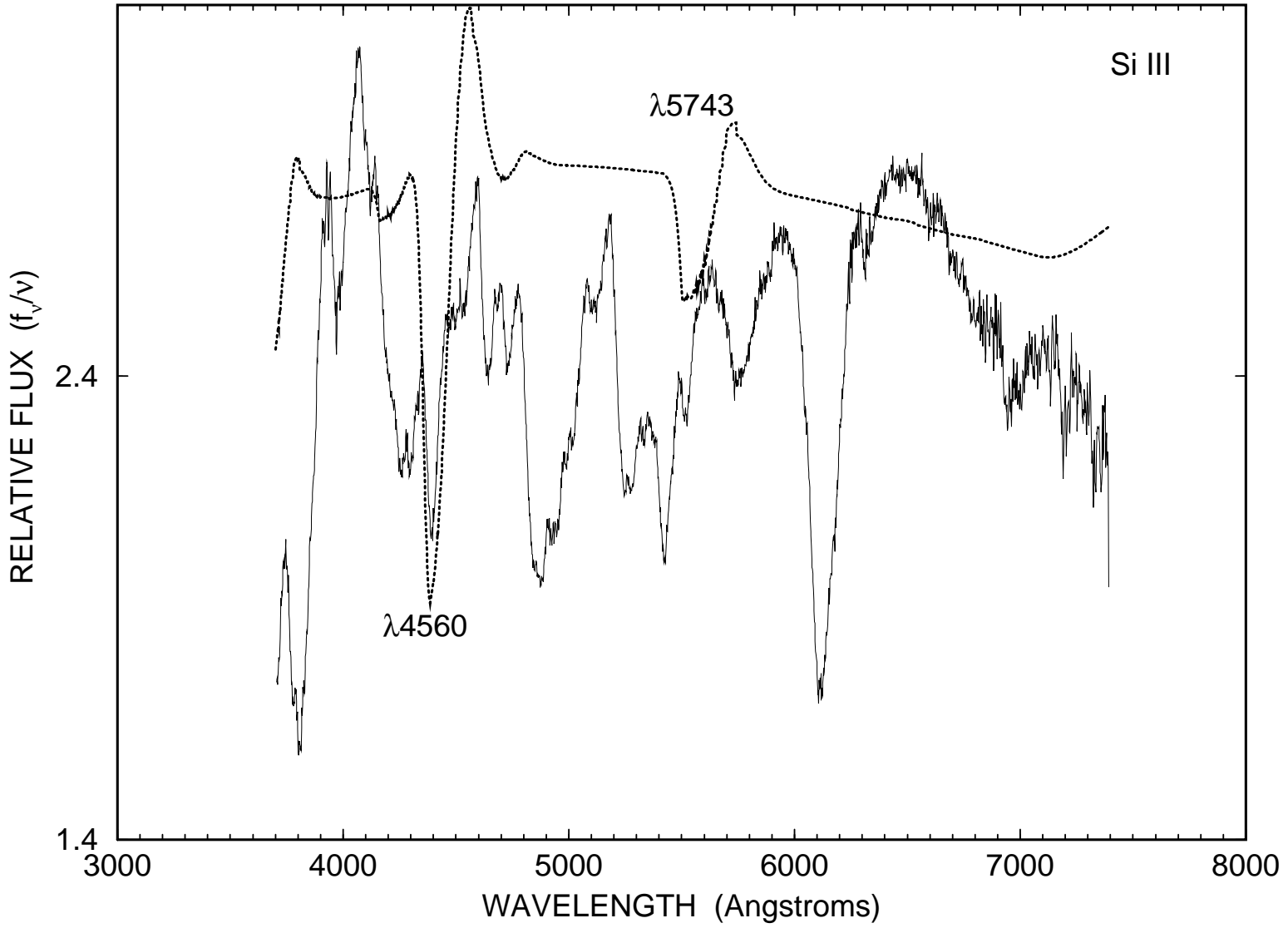


Fig. 14.— Like Fig. 10 but with only lines of Si III in the synthetic spectrum.

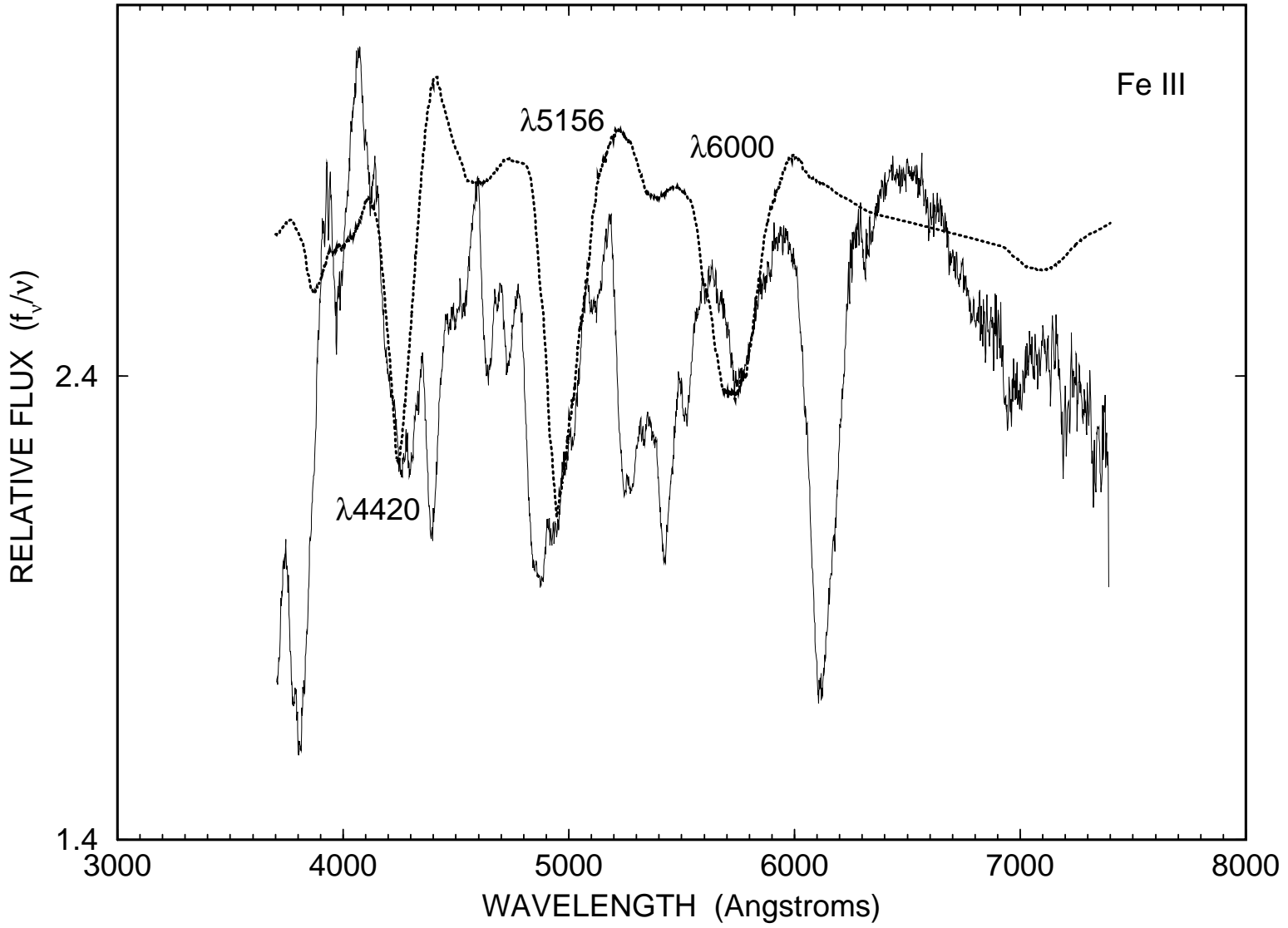


Fig. 15.— Like Fig. 10 but with only lines of Fe III in the synthetic spectrum.

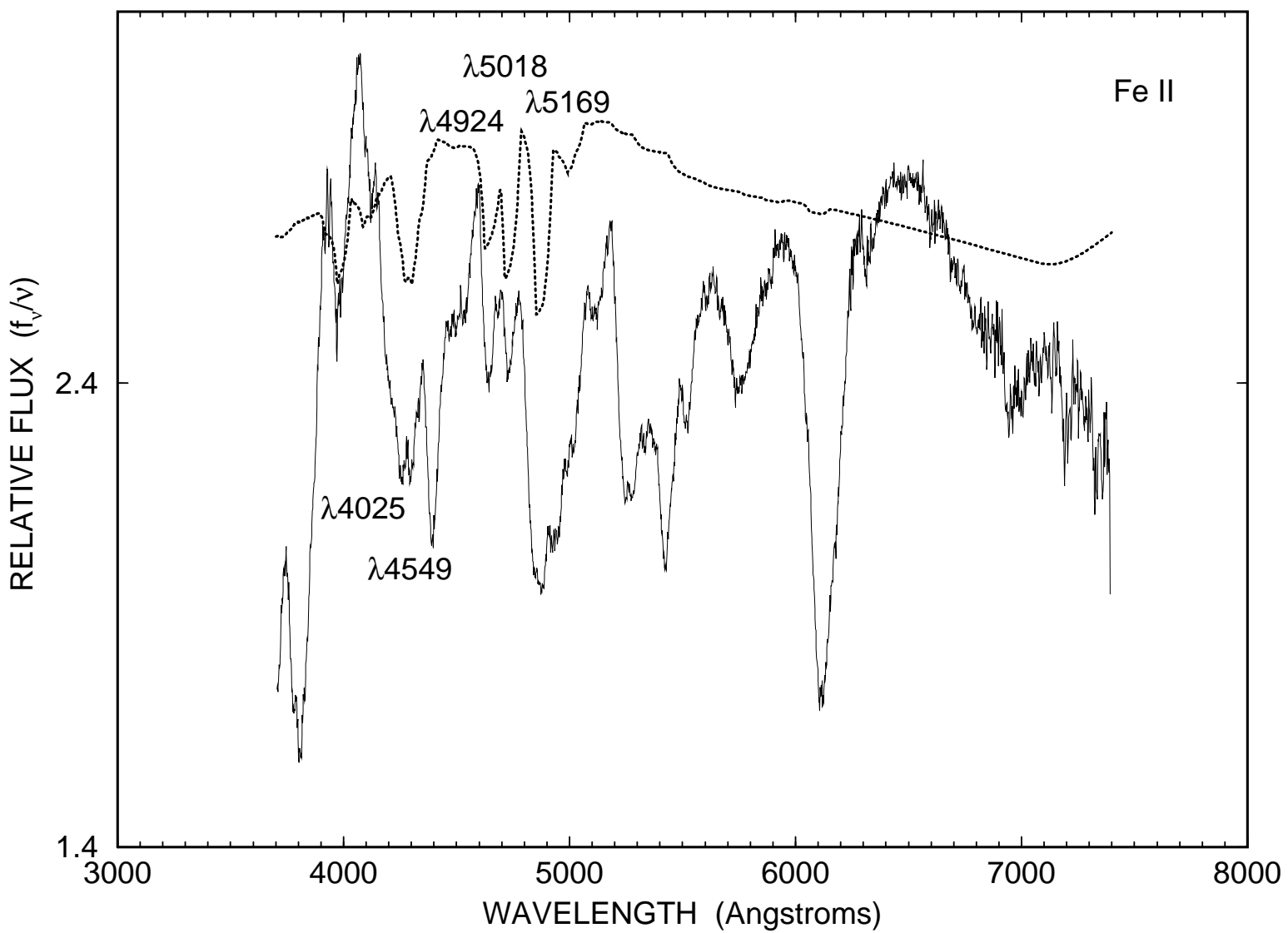


Fig. 16.— Like Fig. 10 but with only lines of Fe II in the synthetic spectrum.

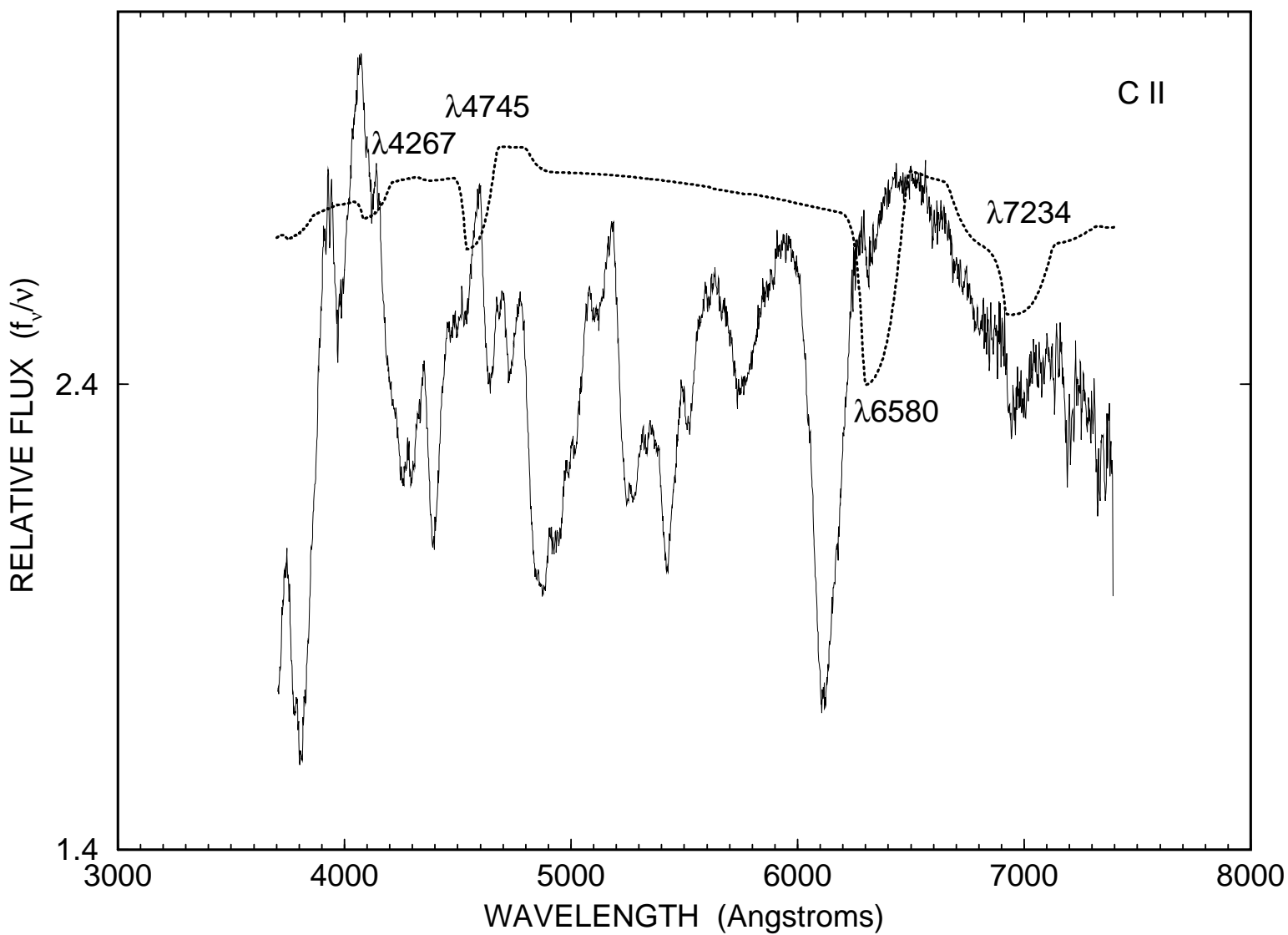


Fig. 17.— Like Fig. 10 but with only lines of C II in the synthetic spectrum.



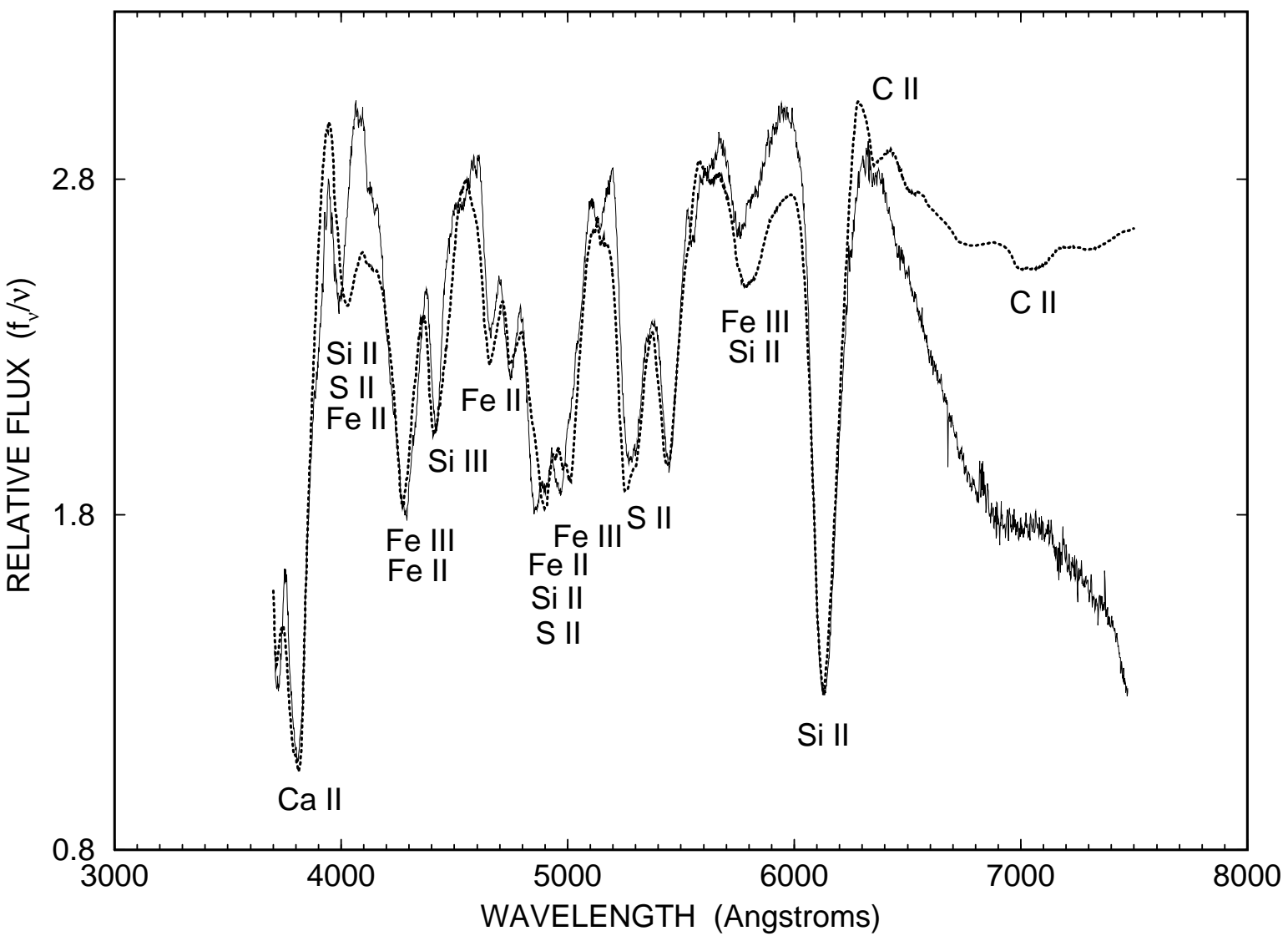


Fig. 18.— Comparison of the 0 day spectrum of SN 1998aq with a **Synow** synthetic spectrum that has  $v_{phot} = 11,000 \text{ km s}^{-1}$ ,  $T_{bb} = 16,000$ , and contains lines of seven ions.

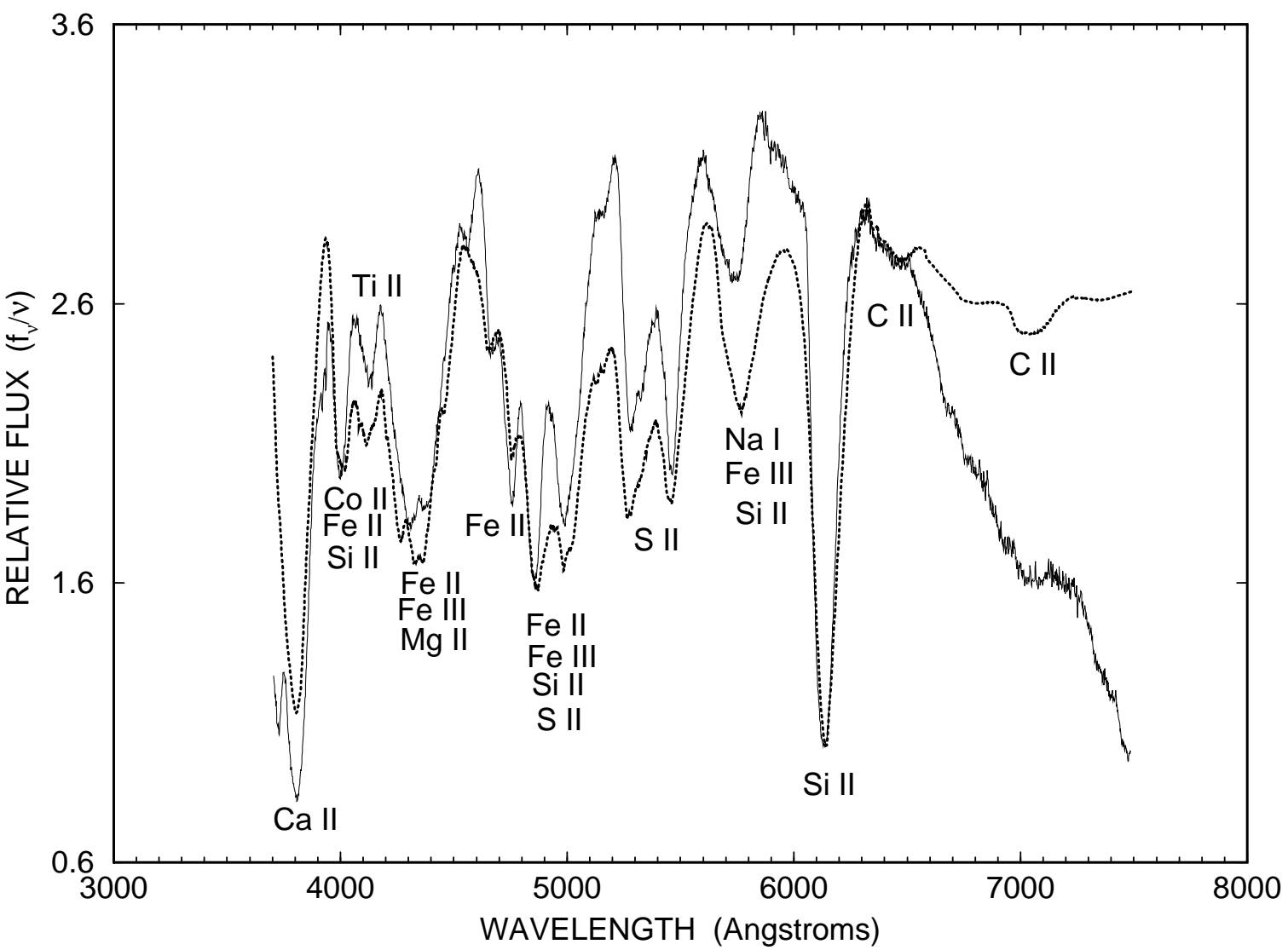


Fig. 19.— Comparison of the 7 day spectrum of SN 1998aq with a **Synow** synthetic spectrum that has  $v_{phot} = 11,000 \text{ km s}^{-1}$ ,  $T_{bb} = 16,000$ , and contains lines of ten ions.

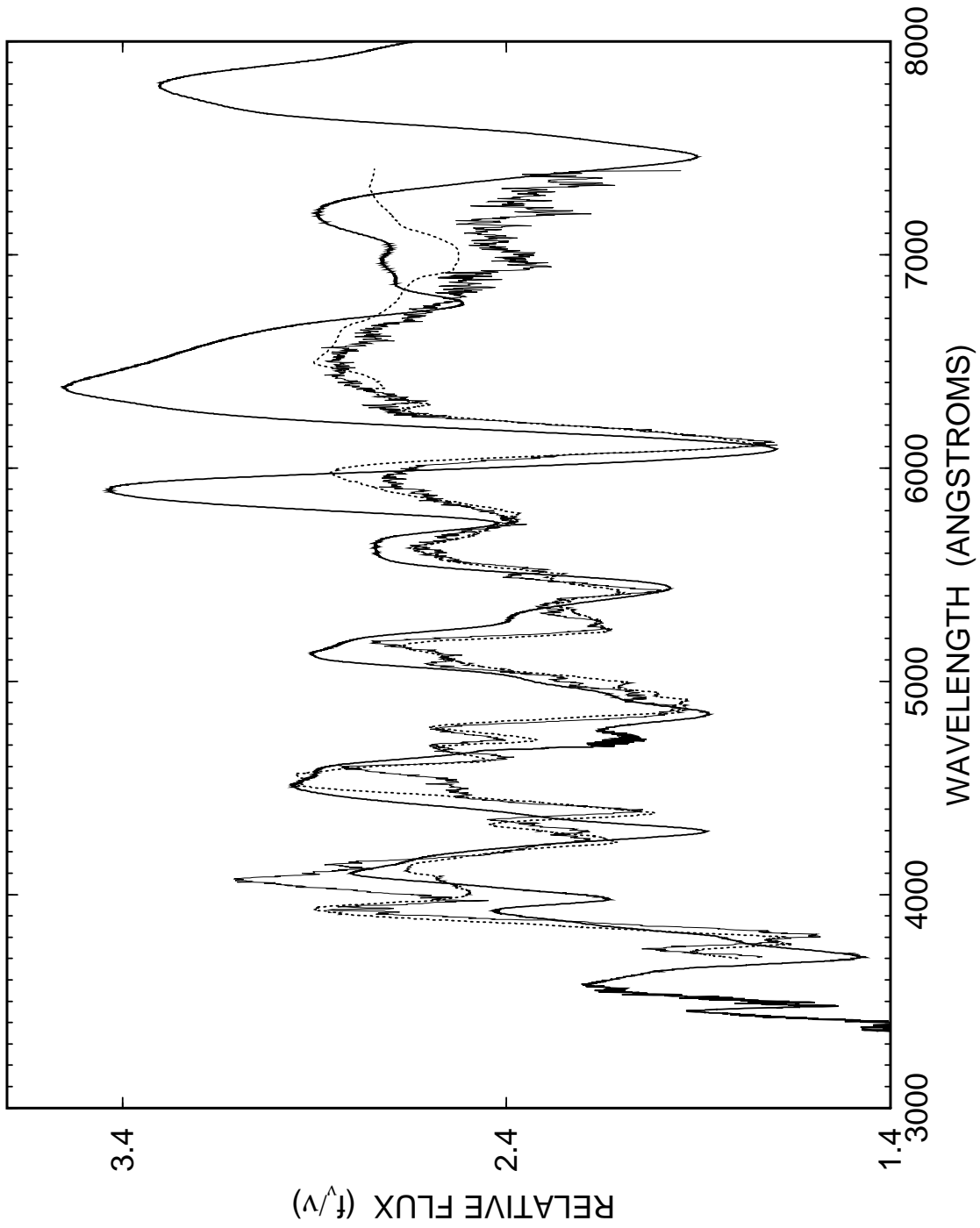


Fig. 20.— Like Fig.10, but including a PHOENIX synthetic spectrum (smooth solid line) for model W7 at 11 days after explosion, from Lentz et al. (2001).

Table 1. JOURNAL OF OBSERVATIONS

UT Date	Julian Day	Tel.	Range (Å)	Res. (Å)	P.A. (°)	Par. (°)	Air.	Flux Std.	Sky	See. (")	Slit (")	Exp. (s)	Observer(s)
1998-04-18.28	2450921.78	FLWO	3720.00-7420.5	7.0	90.00	149.67	1.12	Feige34	clear	1-2	3	900	P Berlind / M Calk
1998-04-19.26	2450922.76	FLWO	3270-7140	7.0	90.00	163.01	1.10	Feige110	clear	2	3	900	P Berlind / M Calk
1998-04-24.36	2450927.86	FLWO	4080.00-6080.2	7.0	110.00	104.63	1.38	Feige34	clear	2	2	1200	Kannappan/Lepore
1998-04-27.29	2450930.79	FLWO	3720-7500	7.0	110.00	130.62	1.17	Feige34	clear	2	2	600	P Berlind
1998-04-28.26	2450931.76	FLWO	3720.00-7510.5	7.0	90.00	148.58	1.12	Feige34	mostly cle	2	3	600	P Berlind
1998-04-29.26	2450932.76	FLWO	3720-7521	7.0	90.00	145.02	1.13	Feige34	mostly cle	2+	3	600	P Berlind
1998-04-30.24	2450933.74	FLWO	3720-7521	7.0	90.00	152.80	1.11	Feige34	mostly cle	2+	3	600	M Calkins
1998-05-01.25	2450934.75	FLWO	3720-7521	7.0	90.00	145.21	1.13	Feige34	clear	3	3	600	M Calkins
1998-05-02.23	2450935.73	FLWO	3720-7521	7.0	90.00	158.42	1.10	Feige34	clear	3	3	600	M Calkins
1998-05-03.24	2450936.74	FLWO	3720-7515	7.0	90.00	148.00	1.12	Feige34	mostly cle	1-2	3	600	P Berlind
1998-05-04.26	2450937.76	FLWO	3720-7512	7.0	90.00	136.26	1.15	Feige34	lots of ci	1-2	3	600	P Berlind
1998-05-16.17	2450949.67	FLWO	3720-7540.5	7.0	90.00	176.89	1.09	Feige34	mostly cle	1-2	3	600	P Berlind
1998-05-18.20	2450951.70	FLWO	3720-7540.5	7.0	90.00	151.82	1.11	Feige34	scattered	1	3	600	M. Calkins
1998-05-28.22	2450961.72	FLWO	3720-7540.5	7.0	91.00	122.30	1.21	Feige34	clear	2	3	660	P Berlind
1998-05-29.19	2450962.69	FLWO	3720-7540.5	7.0	91.00	136.41	1.15	Feige34	cirrus to	2-3	3	660	P Berlind
1998-05-31.20	2450964.70	FLWO	3720-7540.5	7.0	91.00	131.81	1.17	Feige34	cirrus all	2	3	900	M Calkins
1998-06-02.23	2450966.73	FLWO	3720-7540.5	7.0	91.00	113.20	1.27	BDp284211	Clear	3	3	600	M Calkins
1998-06-17.17	2450981.67	FLWO	3720-7540.5	7.0	90.00	123.89	1.21	BDp284211	Clear	1-2	3	900	B. Carter
1998-06-21.18	2450985.68	FLWO	3720-7540.5	7.0	90.00	112.71	1.28	BDp284211	Clear	1-2	3	900	M. Calkins
1998-06-24.19	2450988.69	FLWO	3720-7540.5	7.0	90.00	106.38	1.35	BDp284211	cirrus	1-2	3	900	P Berlind
1998-06-26.19	2450990.69	FLWO	3720-7540.5	7.0	90.00	104.67	1.36	BDp284211	hazy but c	1-2	3	720	P Berlind/K Rines
1998-06-29.17	2450993.67	FLWO	3720-7540.5	7.0	90.00	106.92	1.34	BDp284211	hazy but c	1-2	3	900	K Rines
1998-07-02.17	2450996.67	FLWO	3720-7540.5	7.0	90.00	103.76	1.37	BDp284211	clear!	2+	3	660	P Berlind

Table 1—Continued

UT Date	Julian Day	Tel.	Range (Å)	Res. (Å)	P.A. (°)	Par. (°)	Air.	Flux Std.	Sky	See. (")	Slit (")	Exp. (s)	Observer(s)
1998-07-15.21	2451009.71	FLWO	3720-7540.5	7.0	90.00	82.10	1.92	BDp284211	hazy	2	3	1200	P Berlind
1998-07-18.18	2451012.68	FLWO	3720-7540.5	7.0	90.00	87.61	1.67	BDp284211	major buil		3	600	M Calkins
1998-07-27.17	2451021.67	FLWO	3720-7540.5	7.0	90.00	82.81	1.86	BDp284211	a few scat	2	3	900	P Berlind
1998-11-24.54	2451142.04	FLWO	3720-7540.5	7.0	90.00	-114.52	1.20	Feige34	clear	1+	3	1200	K Rines, J. Huchra
1998-11-24.54	2451142.04	FLWO	3720-7540.5	7.0	90.00	-119.80	1.18	Feige34	clear	1+	3	900	K Rines, J. Huchra
1998-12-14.53	2451162.03	FLWO	3720-7540.5	7.0	59.00	-139.75	1.11	Feige34	clear	1-2	3	1200	M Calkins, A Mahda
1998-12-14.55	2451162.05	FLWO	3720-7540.5	7.0	59.00	-148.65	1.10	Feige34	clear	1-2	3	1200	M Calkins, A Mahda
1998-12-24.53	2451172.03	FLWO	3720-7540.5	7.0	90.00	-157.34	1.09	Feige34	cirrus	2	3	1200	M Calkins
1998-12-24.55	2451172.05	FLWO	3720-7540.5	7.0	90.00	-167.64	1.09	Feige34	cirrus	2	3	1200	M Calkins

Table 2. Input Parameters for Figure 10

ion	$\lambda(\text{ref})$	$\tau(\text{ref})$	$v_{min}$	$T_{exc}$
Si II	$\lambda 6347$	3.5		8000
S II	$\lambda 5454$	1.6		10000
Ca II	$\lambda 3934$	6.0		5000
Si III	$\lambda 4553$	3.0		14000
Fe III	$\lambda 5156$	1.3		16000
Fe II	$\lambda 5018$	0.4	20000	7000
C II	$\lambda 6578$	0.9	14000	12000

Table 3. Input Parameters for Figure 18

ion	$\lambda(\text{ref})$	$\tau(\text{ref})$	$v_{min}$	$T_{exc}$
Si II	$\lambda 6347$	4.0	12000	8000
S II	$\lambda 5454$	1.5	12000	10000
Ca II	$\lambda 3934$	30		5000
Si III	$\lambda 4553$	2.2		14000
Fe III	$\lambda 5156$	1.7		14000
Fe II	$\lambda 5018$	0.4	18000	7000
C II	$\lambda 6578$	0.5		12000

Table 4. Input Parameters for Figure 19

ion	$\lambda(\text{ref})$	$\tau(\text{ref})$	$v_{min}$	$T_{exc}$
Si II	$\lambda 6347$	12		8000
S II	$\lambda 5454$	1.8		10000
Ca II	$\lambda 3934$	40		5000
Fe III	$\lambda 5156$	1.2		14000
Fe II	$\lambda 5018$	2.0		7000
Fe II	$\lambda 5018$	2.0	18000	7000
C II	$\lambda 6578$	0.9		12000
Mg II	$\lambda 4481$	1.0		12000
Na I	$\lambda 5890$	0.5		12000
Co II	$\lambda 4161$	1.0	14000	12000
Ti II	$\lambda 4550$	0.2	14000	6000